



The discovery of purine-based agents targeting triple-negative breast cancer and the α B-crystallin/VEGF protein–protein interaction

Nelly A. Fosu-Mensah^{1,2} · Wen Jiang² · Andrea Brancale¹ · Jun Cai² · Andrew D. Westwell¹

Received: 22 June 2018 / Accepted: 8 December 2018
© The Author(s) 2018

Abstract

Oestrogen receptor-negative breast cancer, particularly subtypes such as triple-negative breast cancer (TNBC, around 10–15% of cases), are characterised by poor long-term survival, poor response to therapy and early progression to metastasis. Purine-based compounds represent a privileged scaffold in anticancer drug design, with several clinically approved and experimental agents in clinical development comprising a purine core structure. In this study, a series of new purine-based compounds were synthesised; seven of the new analogues were found to significantly reduce the in vitro viability of TNBC cell lines (MDA-MB-231 and MDA-MB-436) with IC₅₀ values of ≤ 50 μ M. In previous work, we have proposed a new concept for targeting angiogenesis driving TNBC progression, by disrupting the protein–protein interaction between the molecular chaperone α B-crystallin (CRYAB) and VEGF. Since previous clinical studies applying anti-VEGF therapy to TNBC patients have met with limited success, we were interested to test our most promising purine analogues against CRYAB/VEGF, using a custom-designed cell-based CRYAB/VEGF₁₆₅ interaction assay platform. Analogues **4e** and **4f** significantly reduced the interaction between CRYAB/VEGF₁₆₅, and compound **4e** (100 μ M) was also found to decrease the levels of soluble VEGF expressed by MDA-MB-231 cells by 40%. In conclusion, these promising early activity profiles warrant further investigation to validate this concept.

Keywords Triple-negative breast cancer · Anticancer · Purines · α B-crystallin · VEGFR

Introduction

Triple-negative breast cancer (TNBC) represents an important and unmet clinical challenge, accounting for around 10–15% of all newly diagnosed breast cancer cases. TNBC is classified as a subpopulation of invasive

breast cancer characterised by the lack of expression of the oestrogen receptor (ER), progesterone receptor (PR) and human epidermal growth factor receptor 2 (HER2) (Fosu-Mensah et al. 2015; Lehmann et al. 2011; Mayer et al. 2014). As a subset of breast cancer cases, TNBC is also a “disease of the young”, as it frequently affects premenopausal women of minority background, including black and Hispanic women. It is an aggressive disease associated with high histological grade, increased risk of recurrence and metastatic spread and poor prognosis. Currently, the standard of care treatment for TNBC patients involves the use of cytotoxic chemotherapy (e.g., taxanes). However, this treatment lacks long-term efficacy.

Angiogenesis, the development of new blood vessels from existing vasculature, is essential for early stage tumourigenesis and metastasis. This process is regulated by several pro-angiogenic factors, including vascular endothelial growth factor (VEGF). TNBC is highly vascularised as a result of upregulation of intra-tumoural VEGF levels, which in turn is associated with poor prognosis. In this regard, anti-angiogenic therapies were evaluated clinically

Supplementary information The online version of this article (<https://doi.org/10.1007/s00044-018-2275-9>) contains supplementary material, which is available to authorized users.

✉ Jun Cai
Juncai.284@gmail.com

✉ Andrew D. Westwell
WestwellA@cf.ac.uk

¹ Cardiff School of Pharmacy and Pharmaceutical Science, Cardiff University, Redwood Building, King Edward VII Avenue, Cardiff CF10 3NB Wales, UK

² Cardiff China Medical Research Collaborative, Cardiff University School of Medicine, Henry Wellcome Building, Heath Park, Cardiff CF14 4XN Wales, UK

as potential targeted therapies in TNBC albeit not successfully in terms of long-term survival. Bevacizumab is an anti-angiogenic antibody that has been used in combination with chemotherapy and was first investigated as a therapeutic option due to enhanced angiogenesis in TNBC presentations (Steeg 2006; Kim et al. 2004). This therapy showed promising results in early clinical trials, however, meta-analysis of clinical trial data showed no beneficial effect on overall survival rates (O'Shaughnessy et al. 2009; von Minckwitz et al. 2012; Bear et al. 2012). Most patients were non-responsive to the therapy, while patients who showed initial response eventually developed resistance and relapsed disease. Moreover, in 2011 the FDA revoked its approval of bevacizumab for breast cancer therapy due to reported adverse side effects (Goozner 2011; Ranpura et al. 2011; O'Reilly et al. 2015). There are currently no molecularly targeted therapies that are effective against TNBC in the clinical setting, and therefore there is a high unmet medical need for the development of new effective and efficacious therapies for this poor prognosis patient group (Fosu-Mensah et al. 2015; Chen et al. 2014).

Given the high priority afforded to the further study and treatment of this disease, TNBC has been the subject of intense gene array profiling studies. These studies identified new molecular targets including but not limited to basal epithelial proteins, such as cytokeratin 5 and 6, CK14, CK17, P-cadherin, p53 mutations, epidermal growth factor receptor (EGFR) and α B-crystallin (Lehmann et al. 2011). Ultimately, these studies will provide potential therapeutic targets for drug discovery programmes. Since many of the newly identified TNBC therapeutic targets have established therapies in other disease settings, there are presently numerous clinical studies underway to assess their efficacy in TNBC.

An interesting TNBC-associated target under investigation within our laboratory is α B-crystallin (CRYAB, HspB5). CRYAB is a member of the mammalian small heat-shock protein family that function as molecular chaperones to modulate cell proteostasis, and consequently, cell survival by suppressing aggregation of denatured proteins in stress-induced environments (Tsang et al. 2012; Arrigo et al. 2007; Garrido et al. 2012). CRYAB is ubiquitously expressed in many tissues with varying functions, and upregulation of this protein is observed in many disease pathologies, including neuropathy, myopathy, ischaemia/reperfusion, cataract and various solid tumours (gliomas, prostate, ovarian, colon, liver, head and neck cancer) (Ruan et al. 2011). CRYAB represents a promising therapeutic target owing to its diverse functions as a molecular chaperone. Studies in breast cancers have provided compelling clinical data that showed that CRYAB is constitutively expressed in the most aggressive phenotypes of the disease, including TNBC. Accumulating evidence has revealed that overexpression of CRYAB in TNBC contributes to tumour progression and correlates with

the poor survival rates observed in this aggressive tumour type. This can be attributed to its critical role as a metastatic and anti-apoptotic regulator. Thus, CRYAB has been evaluated as a potentially important biomarker in TNBC (Tsang et al. 2012; Ruan et al. 2011). Our previous structure-based molecular docking studies identified 3-methylglutamic acid as a small molecule with the potential to inhibit CRYAB/VEGF interaction. 3-Methylglutamic acid was shown to disrupt CRYAB/VEGF₁₆₅ interaction and elicit both in vitro and in vivo antitumour, anti-proliferative and anti-angiogenic effects through downregulation of VEGF signalling (Chen et al. 2014).

In recent years, our laboratory has focused on the discovery of new drug candidates for potential application in the TNBC setting (Chen et al. 2014; Haynes et al. 2016). As part of these efforts, we were attracted to the possibilities associated with purine-based compounds, given their long and distinguished history in cancer drug development, including clinically approved anti-leukaemia drugs such as fludarabine (Rodriguez 1994) and clofarabine (Ghanem et al. 2010). Purines represent a privileged heterocycle in drug design, given the ability of purine analogues to bind tightly within hydrophobic folds and inhibit a range of key enzyme targets, such as members of the diverse protein kinase, sulfatase and phosphorylase families. For example, roscovitine (Seliclib) is a cyclin-dependent kinase inhibitory purine analogue in clinical development in a range of cancer, infectious disease and anti-inflammatory settings (De Azevedo et al. 1997). The specific sub-class of thiopurine analogues, such as 6-mercaptopurine and thioguanine, are also used as standard cancer chemotherapeutic agents, principally as anti-leukaemic drugs (Sahasranaman et al. 2008). Figure 1 shows the chemical structures of selected purine analogues in clinical use or advanced development.

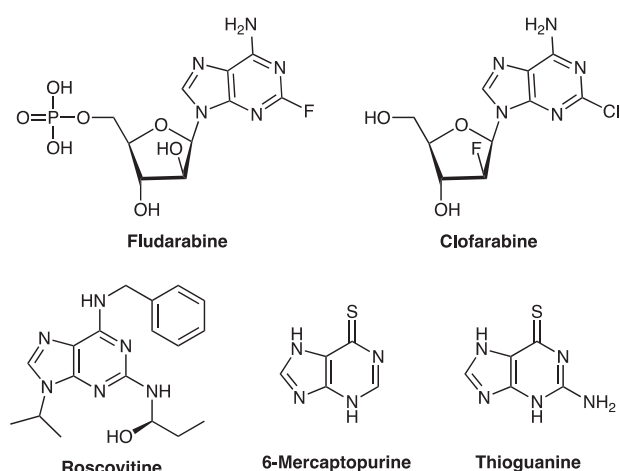


Fig. 1 Anticancer purine analogues in clinical use or advanced development

During our previous work on the identification of 3-methylglutamic acid in disrupting CRYAB/VEGF₁₆₅ interaction (Chen et al. 2014), we noted that the thioguanine core structure was also able to potentially bind within the protein–protein interface binding pocket. In this paper, we extend our studies on the identification of novel chemical scaffolds active in models of TNBC through the synthesis and in vitro antitumour evaluation of a series of substituted thiopurines, and test their potential as CRYAB/VEGF inhibitors.

Materials and methods

All solvents and reagents were used as obtained from commercial sources unless otherwise indicated. Final purification of target compounds was carried out by silica gel column chromatography using CH₂Cl₂/MeOH as eluent. Compound purity was established using ¹H and ¹³C NMR, alongside accurate mass spectrometry. ¹H NMR and ¹³C NMR spectra were recorded in the appropriate deuterated solvents with a Bruker Avance DPX500 spectrometer operating at 500 MHz. Chemical shifts (δ) are reported in parts per million (ppm) using the following abbreviations: s, singlet; d, doublet; t, triplet; q, quartet; quin, quintet; sex, sextet; sep, septet; m, multiplet; br, broad, app.t, apparent triplet. All coupling constants are reported in Hz. Mass spectra were recorded with a Bruker microTOF mass spectrometer using electrospray ionisation (ESI) conditions, or provided as a service at the National Mass Spectrometry Facility at Swansea University, UK. Synthetic procedures and analytical/spectroscopic data for intermediate compounds can be found in Supplementary Information.

General methods for the alkylation of purines

Alkylation method 1

Substituted purine compound (1.0 eq) and potassium carbonate (1.1 eq) were dissolved in DMF (5 mL) at r.t. for 5 min. Bromoethane (1.2 eq) was added dropwise, then the reaction stirred for 3–18 h, after which the reaction was quenched with cold water resulting in precipitation. The precipitate was filtered and washed with water. If no precipitate formed, the product was extracted with chloroform or ethyl acetate, dried over sodium sulphate and concentrated under reduced pressure.

Alkylation method 2

Substituted purine compound (1.0 eq) were dissolved in 1 M potassium hydroxide (1.1 eq). Bromoethane (1.2 eq) was

added dropwise, then the reaction stirred for 3–5 h. On completion of the reaction, the product was precipitated with acetic acid, filtered, washed with water and dried.

Alkylation method 3

Substituted purine compound (1.0 eq) and 1,8-diazabicyclo[5.4.0]undec-7-ene (1.1 eq) were dissolved in DMF at r.t. for 5 min. The alkyl halide (1.2 eq) was added dropwise, then the reaction stirred for 3–5 h. The reaction was then quenched with cold water resulting in precipitation. The precipitate was filtered, washed with water and dried prior to purification by column chromatography.

2,6-bis(ethylthio)-7H-purin-8(9H)-one (4a)

According to general method 3 with 2,6-dimercapto-7H-purin-8(9H)-one (200 mg, 1.0 mmol), DMF (2 mL), DBU (0.15 mL, 1.0 mmol) and bromoethane (0.14 mL, 2.0 mmol) The product was purified by column chromatography with CH₂Cl₂/MeOH 90:10 as an eluent to afford a white solid of yield 90 mg, 35%. ¹H-NMR (500 MHz, DMSO-*d*₆): δ 11.70 (s, br, 1H, NH), 11.16 (s, br, 1H, NH), 3.24 (q, 2H, *J* = 7.5 Hz, SCH₂), 3.09 (q, 2H, *J* = 7.5 Hz, SCH₂), 1.32 (td, 6H, *J*₁ = 7.5 Hz, *J*₂ = 3.0 Hz, CH₃). ¹³C-NMR (500 MHz, DMSO-*d*₆): δ 161.45 (C2), 153.78 (C6), 149.40 (C8), 144.08 (C4), 116.81 (C5), 25.09 (SCH₂), 23.39 (SCH₂), 15.64 (CH₃), 15.28 (CH₃). *m/z* (FTMS + ESI) = Found [M]⁺ (C₉H₁₂N₄OS₂) 256.9068 requires 256.3420.

2,6-bis(methylthio)-7H-purin-8(9H)-one (4b)

According to the general method 3 with 2,6-dimercapto-7H-purin-8(9H)-one (200 mg, 1.0 mmol), DMF (2 mL), DBU (0.15 mL, 1.0 mmol) and iodomethane (0.12 mL, 2.0 mmol). The product was purified by column chromatography with CH₂Cl₂/MeOH 90:10 as an eluent to afford a white solid of yield 110 mg, 48%. ¹H-NMR (500 MHz, DMSO-*d*₆): δ 11.75 (s, br, 1H, NH), 11.23 (s, br, 1H, NH), 2.60 (s, 3H, SCH₃), 2.51 (s, 3H, SCH₃). ¹³C-NMR (500 MHz, DMSO-*d*₆): δ 161.98 (C2), 153.78 (C6), 149.13 (C8), 144.58 (C4), 116.59 (C5), 14.24 (SCH₃), 11.82 (SCH₃). *m/z* (FTMS + ESI) = Found [M+H]⁺ (C₇H₈N₄OS₂) 229.0212 requires 228.2880.

2,6-bis(propylthio)-7H-purin-8(9H)-one (4c)

According to the general method 3 with 2,6-dimercapto-7H-purin-8(9H)-one (100 mg, 0.5 mmol), DMF (2 mL), DBU (0.08 mL, 0.5 mmol) and 1-bromopropane (0.09 mL, 1.0 mmol). The product was purified by column chromatography with CH₂Cl₂/MeOH 90:10 as an eluent to afford a light yellow solid of yield 100 mg, 70%. ¹H-NMR (500

MHz, DMSO- d_6): δ 11.69 (s, br, 1H, NH), 11.15 (s, br, 1H, NH), 3.21 (t, 2H, $J = 7.0$ Hz, SCH₂), 3.06 (t, 2H, $J = 7.0$ Hz, SCH₂), 1.65–1.73 (m, 4H, CH₂), 0.97–1.00 (m, 6H, CH₃). ¹³C-NMR (500 MHz, DMSO- d_6): δ 161.45 (C2), 153.78 (C6), 149.37 (C8), 144.07 (C4), 116.82 (C5), 32.68 (SCH₂), 30.64 (SCH₂), 23.41 (CH₂), 23.02 (CH₂), 13.79 (CH₃), δ 13.63 (CH₃). m/z (FTMS + ESI) = Found [M]⁺ (C₁₁H₁₆N₄OS₂) 284.9649 requires 284.3960.

2,6-bis(isobutylthio)-7H-purin-8(9H)-one (4d)

According to the general method 3 with 2,6-dimercapto-7H-purin-8(9H)-one (200 mg, 1.0 mmol), DMF (2 ml), DBU (0.15 ml, 1.0 mmol) and 1-bromo-2-methylpropane (0.22 ml, 2.0 mmol). The product was purified by column chromatography with CH₂Cl₂/MeOH 90:10 as eluent to afford a light yellow solid of yield 90 mg, 29%. ¹H-NMR (500 MHz, DMSO- d_6): δ 11.67 (s, br, 1H, NH), 11.17 (s, br, 1H, NH), 3.18 (d, 2H, $J = 7.0$ Hz, SCH₂), 3.02 (d, 2H, $J = 7.0$ Hz, SCH₂), 1.92 (sep, 2 × 1H, $J = 7.0$ Hz, CH), 1.00 (d, 12H, $J = 7.0$ Hz, CH₃). ¹³C-NMR (500 MHz, DMSO- d_6): δ 161.45 (C2), 153.81 (C6), 149.36 (C8), 144.00 (C4), 116.81 (C5), 39.20 (SCH₂), 36.86 (SCH₂), 28.80 (CH), 28.38 (CH), 22.21 (CH₃), 22.01 (CH₃). m/z (FTMS + ESI) = Found [M+H]⁺ (C₁₃H₂₀N₄OS₂) 313.0257 requires 312.4500.

2,6-bis(benzylthio)-7H-purin-8(9H)-one (4e)

According to the general method 3 with 2,6-dimercapto-7H-purin-8(9H)-one (100 mg, 0.5 mmol), DMF (2 ml), DBU (0.08 ml, 0.5 mmol) and benzyl bromide (0.11 ml, 1.0 mmol). The product was purified by column chromatography with CH₂Cl₂/MeOH 90:10 as an eluent to afford an off white solid of yield 140 mg, 74%. ¹H-NMR (500 MHz, DMSO- d_6): δ 11.81 (s, br, 1H, NH), 11.76 (s, br, 1H, NH), 7.41 (d, 2H, $J = 7.2$ Hz, CH_{Bz}), 7.37 (d, 2H, $J = 7.2$ Hz, CH_{Bz}), 7.29–7.32 (m, 4H, CH_{Bz}), 7.23–7.27 (m, 2H, CH_{Bz}), 4.51 (s, 2H, SCH₂), 4.40 (s, 2H, SCH₂). ¹³C-NMR (500 MHz, DMSO- d_6): δ 161.12 (C2), 153.77 (C6), 149.55 (C8), 143.52 (C4), 138.24 (C_{Bz}), 138.02 (C_{Bz}), 129.34 (CH_{Bz}), 129.23 (CH_{Bz}), 128.97 (CH_{Bz}), 128.89 (CH_{Bz}), 127.70 (CH_{Bz}), 127.50 (CH_{Bz}), 116.76 (C5), 34.95 (CH₂), 32.73 (CH₂). m/z (FTMS + ESI) = Found [M+H]⁺ (C₁₉H₁₆N₄OS₂) 381.0796 requires 380.4840.

2,6-bis(phenethylthio)-7H-purin-8(9H)-one (4f)

According to the general method 3 with 2,6-dimercapto-7H-purin-8(9H)-one (100 mg, 0.5 mmol), DMF (2 ml), DBU (0.08 ml, 0.5 mmol) and 2-bromoethyl benzene (0.14 ml, 1.0 mmol). The product was purified by column chromatography with CH₂Cl₂/MeOH 90:10 as an eluent to afford a white solid of yield 100 mg, 49%. ¹H-NMR (500 MHz, DMSO- d_6): δ 11.78 (s, br, 1H, NH), 11.20 (s, br, 1H, NH),

7.19–7.31 (m, 10H, H_{Bz}), 3.53 (t, 2H, $J = 7.5$ Hz, SCH₂), 3.36 (t, 2H, $J = 7.5$ Hz, SCH₂), 2.95 (t, 4H, $J = 7.5$ Hz, CH₂). ¹³C-NMR (500 MHz, DMSO- d_6): δ 161.35 (C2), 153.80 (C6), 149.45 (C8), 143.86 (C4), 140.72 (C_{Bz}), 140.32 (C_{Bz}), 128.98 (CH_{Bz}), 128.84 (CH_{Bz}), 128.82 (CH_{Bz}), 126.82 (CH_{Bz}), 126.72 (CH_{Bz}), 116.95 (C5), 35.82 (CH₂), 35.60 (CH₂), 32.04 (SCH₂), 30.05 (SCH₂). m/z (FTMS + ESI) = Found [M+H]⁺ (C₂₁H₂₀N₄OS₂) 409.1150 requires 408.5380.

2,6-bis((3-phenylpropyl)thio)-7H-purin-8(9H)-one (4g)

According to the general method 3 with 2,6-dimercapto-7H-purin-8(9H)-one (100 mg, 0.5 mmol), DMF (2 ml), DBU (0.08 ml, 0.5 mmol) and 1-bromo-3-phenylpropane (0.15 ml, 1.0 mmol). The product was purified by column chromatography with CH₂Cl₂/MeOH 90:10 as an eluent to afford an off-white solid of yield 110 mg, 50%. ¹H-NMR (500 MHz, DMSO- d_6): δ 11.71 (s, br, 1H, NH), 11.17 (s, br, 1H, NH), 7.25–7.29 (m, 4H, H_{Ph}), 7.16–7.19 (m, 6H, H_{Ph}), 3.21 (t, 2H, $J = 7.5$ Hz, SCH₂), 3.06 (t, 2H, $J = 7.5$ Hz, SCH₂), 2.69 (t, 4H, $J = 7.0$ Hz, CH₂), 1.92–1.98 (m, 4H, CH₂). ¹³C-NMR (500 MHz, DMSO- d_6): δ 161.33 (C2), 153.78 (C6), 149.44 (C8), 143.88 (C4), 141.67 (C_{Ph}), 141.47 (C_{Ph}), 128.84 (CH_{Ph}), 128.82 (CH_{Ph}), 128.76 (CH_{Ph}), 128.74 (CH_{Ph}), 126.38 (CH_{Ph}), 126.33 (CH_{Ph}), 116.97 (C5), 34.70 (CH₂), 34.57 (CH₂), 31.51 (CH₂), 31.17 (CH₂), 30.33 (SCH₂), 28.40 (SCH₂). m/z (FTMS + ESI) = Found [M+H]⁺ (C₂₃H₂₄N₄OS₂) 437.2875 requires 436.5920.

9-ethyl-2,6-bis(ethylthio)-8,9-dihydro-7H-purine-8-thiol (6a)

According to the general method 3 with 2,6-dimercapto-7,9-dihydro-8H-purine-8-thione (100 mg, 0.46 mmol), DMF (2 ml), DBU (0.07 ml, 0.46 mmol) and bromoethane (0.07 ml, 0.92 mmol). The product was purified by column chromatography with CH₂Cl₂/MeOH 95:5 as an eluent to afford a light yellow solid of yield 40 mg, 29%. ¹H-NMR (500 MHz, DMSO- d_6): δ 13.21 (s, br, 1H, NH), 3.27–3.31 (m, 4H, CH₂), 3.10–3.16 (m, 2H, CH₂), 1.32–1.39 (m, 9H, CH₃). ¹³C-NMR (500 MHz, DMSO- d_6): δ 169.99 (C8), 163.58 (C2), 150.73 (C6), 147.44 (C4), 119.40 (C5), 25.82 (NCH₂), 25.25 (SCH₂), 23.49 (SCH₂), 15.43 (CH₃), 15.29 (CH₃), 15.19 (CH₃). m/z (FTMS + ESI) = Found [M+H]⁺ (C₁₁H₁₆N₄S₃) 301.0609 requires 300.4570.

9-methyl-2,6-bis(methylthio)-7,9-dihydro-8H-purine-8-thione (6b)

According to the general method 3 with 2,6-dimercapto-7,9-dihydro-8H-purine-8-thione (100 mg, 0.46 mmol) DMF

(2 ml), DBU (0.07 ml, 0.46 mmol) and iodomethane (0.06 ml, 0.92 mmol). The product was purified by column chromatography with CH₂Cl₂/MeOH 95:5 as an eluent to afford the tri-substituted product as an off-white solid of yield 40 mg, 17%. ¹H-NMR (500 MHz, DMSO-*d*₆, tri-substituted product): δ 2.54 (s, 3H, CH₃), 2.52 (s, 3H, CH₃), 2.47 (s, 3H, CH₃). ¹³C-NMR (500 MHz, DMSO-*d*₆): δ 163.84 (C8), 163.19 (C2), 156.40 (C6), 148.74 (C4), 133.58 (C5), 14.31 (CH₃), 14.12 (CH₃), 11.56 (CH₃). *m/z* (FTMS + ESI) = Found [M+H]⁺ (C₈H₁₀N₄S₃) 259.0133 requires 258.3760.

The tetra-substituted product (7) was an off-white solid of yield 50 mg, 30%. ¹H-NMR (500 MHz, DMSO-*d*₆, tetra-substituted product): δ 3.85 (s, 3H, NCH₃), 2.75 (s, 3H, NCH₃), 2.64 (s, 3H, SCH₃), 2.54 (s, 3H, SCH₃). ¹³C-NMR (500 MHz, DMSO-*d*₆): δ 162.84 (C8), 156.54 (C2), 153.80 (C6), 151.99 (C4), 128.85 (C5), 33.45 (CH₃), 29.08 (CH₃), 14.09 (CH₃), 11.68 (CH₃). *m/z* (FTMS + ESI) = Found [M+H]⁺ (C₉H₁₂N₄S₃) 273.0334 requires 272.4030.

9-propyl-2,6-bis(propylthio)-8,9-dihydro-7H-purine-8-thiol (6c)

According to general the method 3 with 2,6-dimercapto-7,9-dihydro-8H-purine-8-thione (100 mg, 0.46 mmol), DMF (2 ml), DBU (0.07 ml, 0.46 mmol) and 1-bromopropane (0.08 ml, 0.92 mmol). The product was purified by column chromatography with CH₂Cl₂/MeOH 95:5 as an eluent to afford a light yellow solid of yield 74 mg, 47%. ¹H-NMR (500 MHz, DMSO-*d*₆): δ 3.24–3.29 (m, 4H, SCH₂), 3.08–3.13 (m, 2H, NCH₂), 1.68–1.76 (m, 6H, CH₂), 0.97–1.03 (m, 9H, CH₃). ¹³C-NMR (500 MHz, DMSO-*d*₆): δ 170.03 (C8), 163.56 (C2), 150.72 (C6), 147.41 (C4), 119.47 (C5), 32.88 (SCH₂), 32.82 (SCH₂), 30.69 (NCH₂), 23.20 (CH₂), 23.03 (CH₂), 22.95 (CH₂), 13.78 (CH₃), 13.69 (CH₃), 13.66 (CH₃). *m/z* (FTMS + ESI) = Found [M+H]⁺ (C₁₄H₂₂N₄S₃) 343.1079 requires 342.5380.

9-isobutyl-2,6-bis(isobutylthio)-8,9-dihydro-7H-purine-8-thiol (6d)

According to the general method 3 with 2,6-dimercapto-7,9-dihydro-8H-purine-8-thione (100 mg, 0.46 mmol), DMF (2 ml), DBU (0.07 ml, 0.46 mmol) and 1-bromo-2-methylpropane (0.10 ml, 0.92 mmol). The product was purified by column chromatography with CH₂Cl₂/MeOH 95:5 as an eluent to afford a light yellow solid of yield 80 mg, 45%. ¹H-NMR (500 MHz, DMSO-*d*₆): δ 13.36 (s, br, 1H, NH), 3.22 (dd, 4H, *J* = 6.8 Hz, SCH₂), 3.08 (d, 2H, *J* = 6.8 Hz, NCH₂), 1.90–2.02 (m, 3H, CH), 1.00–1.03 (m, 18H, CH₃). ¹³C-NMR (500 MHz, DMSO-*d*₆): δ 162.43 (C8), 156.04 (C2), 152.58 (C6), 151.88 (C4), 129.41 (C5), 39.51 (S-CH₂), 39.43 (SCH₂), 36.51 (NCH₂), 28.73 (CH), 28.52

(CH), 28.43 (CH), 22.23 (CH₃), 22.08 (CH₃), 21.95 (CH₃). *m/z* (FTMS + ESI) = Found [M+H]⁺ (C₁₇H₂₈N₄S₃) 385.1744 requires 384.6190.

9-benzyl-2,6-bis(benzylthio)-8,9-dihydro-7H-purine-8-thiol (6e)

According to the general method 3 with 2,6-dimercapto-7,9-dihydro-8H-purine-8-thione (100 mg, 0.46 mmol), DMF (2 ml), DBU (0.07 ml, 0.46 mmol) and benzyl bromide (0.11 ml, 0.92 mmol). The precipitate was filtered, washed with water and dried. The product was purified by column chromatography with CH₂Cl₂/MeOH 95:5 as an eluent to afford a light yellow solid of yield 120 mg, 54%. ¹H-NMR (500 MHz, DMSO-*d*₆): δ 13.55 (s, br, 1H, NH), 7.42–7.47 (m, 6H, CH_{Bz}), 7.30–7.33 (m, 6H, CH_{Bz}), 7.24–7.28 (m, 3H, CH_{Bz}), 4.59 (s, 2H, SCH₂), 4.56 (s, br, 2H, NCH₂), 4.46 (s, 2H, SCH₂). ¹³C-NMR (500 MHz, DMSO-*d*₆): δ 162.29 (C8), 155.76 (C2), 152.73 (C6), 151.56 (C4), 138.21 (C_{Bz}), 137.53 (C_{Bz}), 129.47 (CH_{Bz}), 129.40 (CH_{Bz}), 129.28 (CH_{Bz}), 128.99 (CH_{Bz}), 128.95 (CH_{Bz}), 128.91 (CH_{Bz}), 127.97 (CH_{Bz}), 129.41 (C5), 127.66 (CH_{Bz}), 127.53 (CH_{Bz}), 35.24 (SCH₂), 35.13 (SCH₂), 32.38 (NCH₂). *m/z* (FTMS + ESI) = Found [M+H]⁺ (C₂₆H₂₂N₄S₃) 487.3201 requires 486.6700.

9-phenethyl-2,6-bis(phenethylthio)-8,9-dihydro-7H-purine-8-thiol (6f)

According to the general method 3 with 2,6-dimercapto-7H-purine-8(9H)-thione (100 mg, 0.46 mmol) DMF (2 ml), DBU (0.07 ml, 0.46 mmol) and 2-bromoethyl benzene (0.13 ml, 0.92 mmol). The precipitate was filtered, washed with water and dried. The product was purified by column chromatography with CH₂Cl₂/MeOH 95:5 as an eluent to afford a light yellow solid of yield 102 mg, 42%. ¹H-NMR (500 MHz, DMSO-*d*₆): δ 13.43 (s, br, 1H, NH), 7.29–7.34 (m, 12H, CH_{Bz}), 7.21–7.25 (m, 3H, CH_{Bz}), 3.52–3.59 (m, 4H, SCH₂), 3.41–3.44 (m, 2H, NCH₂), 2.99–3.05 (m, 6H, CH₂). ¹³C-NMR (500 MHz, DMSO-*d*₆): δ 162.37 (C8), 156.00 (C2), 152.71 (C6), 151.60 (C4), 140.76 (C_{Bz}), 140.49 (C_{Bz}), 140.21 (C_{Bz}), 129.55 (C5), 129.09 (CH_{Bz}), 129.00 (CH_{Bz}), 128.87 (CH_{Bz}), 128.82 (CH_{Bz}), 126.91 (CH_{Bz}), 126.84 (CH_{Bz}), 126.73 (CH_{Bz}), 35.71 (SCH₂), 35.57 (SCH₂), 35.33 (NCH₂), 32.62 (SCH₂), 32.25 (SCH₂), 29.79 (NCH₂). *m/z* (FTMS + ESI) = Found [M+H]⁺ (C₂₉H₂₈N₄S₃) 529.15 requires 528.75.

9-(3-phenylpropyl)-2,6-bis((3-phenylpropyl)thio)-8,9-dihydro-7H-purine-8-thiol (6g)

According to the general method 3 with 2,6-dimercapto-7,9-dihydro-8H-purine-8-thione (100 mg, 0.46 mmol) DMF (2 ml), DBU (0.07 ml, 0.46 mmol) and 1-bromo-3-phenyl

propane (0.14 ml, 0.92 mmol). The reaction was quenched with water resulting in precipitation. The precipitate was filtered, washed with water and dried. The product was purified by column chromatography with CH₂Cl₂/MeOH 95:5 as an eluent to afford a light yellow solid of yield 116 mg, 44%. ¹H-NMR (500 MHz, DMSO-*d*₆): δ 13.40 (s, br, 1H, NH), 7.26–7.31 (m, 6H, CH_{Ph}), 7.16–7.24 (m, 9H, CH_{Ph}), 3.26–3.29 (m, 4H, SCH₂), 3.13 (dd, *J*₁ = 7.5 Hz, *J*₂ = 2.5 Hz, 2H, NCH₂), 1.95–2.07 (m, 6H, CH₂). ¹³C-NMR (500 MHz, DMSO-*d*₆): δ 162.33 (C8), 155.96 (C2), 152.66 (C6), 151.66 (C4), 141.68 (C_{Ph}), 141.53 (C_{Ph}), 141.44 (C_{Ph}), 129.54 (C5), 128.84 (CH_{Ph}), 128.83 (CH_{Ph}), 128.79 (CH_{Ph}), 128.77 (CH_{Ph}), 126.39 (CH_{Ph}), 126.37 (CH_{Ph}), 126.34 (CH_{Ph}), 34.70 (SCH₂), 34.62 (SCH₂), 34.39 (NCH₂), 31.35 (SCH₂), 31.15 (SCH₂), 30.97 (NCH₂), 30.87 (SCH₂), 30.54 (SCH₂), 38.00 (NCH₂). *m/z* (FTMS + ESI) = Found [M+H]⁺ (C₃₄H₃₄N₄S₃) 571.2016 requires 570.8320.

General method for the hydrolysis of brominated alkyl-guanines: synthesis of 2-amino-6-hydroxy-9-alkyl-7,9-dihydro-8H-purin-8-ones (13a-g)

A mixture of brominated alkyl-guanine (**12a-g**, 1 eq), sodium acetate (5.3 eq), acetic acid (3 ml) and acetic anhydride (0.5 ml) were heated under reflux and N₂ for 15 h. The reaction was cooled and evaporated to dryness. The resulting residue was suspended in water (5 ml) and the pH adjusted to 13 with 10 M NaOH. The mixture was refluxed for 20 min, cooled and the solid formed collected, triturated with potassium phosphate buffer pH 7.5, filtered and dried.

2-amino-6-hydroxy-9-methyl-7,9-dihydro-8H-purin-8-one (13a)

According to the general method with 2-amino-8-bromo-9-methyl-9H-purin-6-ol (100 mg, 0.41 mmol) and sodium acetate (178 mg, 2.17 mg) to afford a tan solid of yield 62 mg, 63%. ¹H-NMR (500 MHz, DMSO-*d*₆): δ 10.41 (s, 1H, OH), 6.90 (s, br, 2H, NH₂), 3.08 (s, 3H, CH₃). ¹³C-NMR (500 MHz, DMSO-*d*₆): δ 154.69 (C2), 153.02 (C6), 152.08 (C4), 148.78 (C8), 98.55 (C5), 25.90 (CH₃). *m/z* (FTMS + ESI) = Found [M+H]⁺ (C₆H₇N₅O₂) 182.0672 requires 181.1550.

2-amino-9-ethyl-6-hydroxy-7,9-dihydro-8H-purin-8-one (13b)

According to the general method with 2-amino-8-bromo-9-ethyl-9H-purin-6-ol (100 mg, 0.39 mmol) and sodium acetate (170 mg, 2.05 mg) to afford a tan solid of yield 40 mg, 40%. ¹H-NMR (500 MHz, DMSO-*d*₆): δ 10.65 (s, br, 1H, NH), 10.49 (s, 1H, OH), 6.48 (s, br, 2H, NH₂), 3.62 (q, 2H, *J* = 7.0 Hz, NCH₂), 1.16 (t, 3H, *J* = 7.0 Hz, CH₃). ¹³C-NMR (500 MHz, DMSO-*d*₆): δ 153.97 (C2), 152.79 (C6), 151.45 (C4), 148.51 (C8), 98.55 (C5), 41.38 (NCH₂), 11.48

(CH₃). *m/z* (FTMS + ESI) = Found [M+H]⁺ (C₆H₇N₅O₂) 196.0828 requires 195.1820.

2-amino-6-hydroxy-9-propyl-7,9-dihydro-8H-purin-8-one (13c)

According to the general method with 2-amino-8-bromo-9-propyl-9H-purin-6-ol (100 mg, 0.37 mmol) and sodium acetate (160 mg, 1.95 mg) to afford a tan solid of yield 20 mg, 26%. ¹H-NMR (500 MHz, DMSO-*d*₆): δ 10.64 (s, br, 1H, NH), 10.53 (s, 1H, OH), 6.49 (s, br, 2H, NH₂), 3.54 (t, 2H, *J* = 7.5 Hz, NCH₂), 1.60 (sext, 2H, *J* = 7.5 Hz, CH₂), 0.83 (t, 3H, *J* = 7.5 Hz, CH₃). ¹³C-NMR (500 MHz, DMSO-*d*₆): δ 153.97 (C2), 152.79 (C6), 151.45 (C4), 148.51 (C8), 98.55 (C5), 41.38 (NCH₂), 21.99 (CH₂), 11.48 (CH₃). *m/z* (FTMS + ESI) = Found [M+H]⁺ (C₈H₁₁N₅O₂) 210.0986 requires 209.2090.

2-amino-6-hydroxy-9-isobutyl-7,9-dihydro-8H-purin-8-one (13d)

According to the general method with 2-amino-8-bromo-9-isobutyl-9H-purin-6-ol (100 mg, 0.35 mmol) and sodium acetate (152 mg, 1.85 mg) to afford a tan solid of yield 45 mg, 58%. ¹H-NMR (500 MHz, DMSO-*d*₆): δ 10.73 (s, br, 1H, NH), 10.49 (s, 1H, OH), 6.48 (s, br, 2H, NH₂), 3.39 (td, 2H, *J* = 7.5 Hz, NCH₂), 2.10 (sept, 1H, *J*₁ = 7.5 Hz, *J*₂ = 6.5 Hz, CH), 0.82 (d, 6H, *J* = 6.5 Hz, CH₃). ¹³C-NMR (500 MHz, DMSO-*d*₆): δ 154.03 (C2), 153.02 (C6), 151.66 (C4), 148.74 (C8), 98.55 (C5), 46.68 (NCH₂), 27.63 (CH), 20.22 (2xCH₃). *m/z* (FTMS + ESI) = Found [M+H]⁺ (C₉H₁₃N₅O₂) 224.1142 requires 223.2360.

2-amino-9-benzyl-6-hydroxy-7,9-dihydro-8H-purin-8-one (13e)

According to the general method with 2-amino-9-benzyl-8-bromo-9H-purin-6-ol (100 mg, 0.31 mmol) and sodium acetate (135 mg, 1.65 mg) to afford a tan solid of yield 40 mg, 50%. ¹H-NMR (500 MHz, DMSO-*d*₆): δ 10.80 (s, br, 1H, NH), 10.67 (s, 1H, OH), 7.24–7.33 (m, 5H, H_{Bz}), 6.52 (s, br, 2H, NH₂), 4.80 (s, 2H, NCH₂). ¹³C-NMR (500 MHz, DMSO-*d*₆): δ 154.17 (C2), 152.73 (C4), 148.38 (C6), 137.82 (C8), 128.94 (C_{Bz}), 127.67 (CH_{Bz}), 127.42 (CH_{Bz}), 98.74 (C5), 42.60 (NCH₂). *m/z* (FTMS + ESI) = Found [M+H]⁺ (C₁₂H₁₁N₅O₂) 258.0988 requires 257.2530.

2-amino-6-hydroxy-9-phenethyl-7,9-dihydro-8H-purin-8-one (13f)

According to the general method with 2-amino-8-bromo-9-phenethyl-9H-purin-6-ol (100 mg, 0.30 mmol) and sodium acetate (129 mg, 1.57 mg) to afford a tan solid of yield

69 mg, 85%. $^1\text{H-NMR}$ (500 MHz, $\text{DMSO-}d_6$): δ 10.50 (s, 1H, OH), 7.26–7.30 (m, 2H, H_{Bz}), 7.19–7.22 (m, 3H, H_{Bz}), 6.93 (s, br, 4H, NH_2), 3.81–3.88 (m, 2H, CH_2), 2.94–3.00 (m, 2H, CH_2). $^{13}\text{C-NMR}$ (500 MHz, $\text{DMSO-}d_6$): δ 154.66 (C2), 152.66 (C4), 148.69 (C6), 139.01 (C8), 138.84 (C_{Bz}), 129.03 (CH_{Bz}), 128.86 (CH_{Bz}), 126.80 (CH_{Bz}), 98.47 (C5), 34.38 (NCH_2), 30.80 (CH_2). m/z (FTMS + ESI) = Found $[\text{M}+\text{H}]^+$ ($\text{C}_{13}\text{H}_{13}\text{N}_5\text{O}_2$) 272.1146 requires 271.2800.

2-amino-6-hydroxy-9-(3-phenylpropyl)-7,9-dihydro-8H-purin-8-one (13g)

According to the general method with 2-amino-8-bromo-9-(3-phenylpropyl)-9H-purin-6-ol (100 mg, 0.29 mmol) and sodium acetate (125 mg, 1.52 mg) to afford a tan solid of yield 5 mg, 6%. $^1\text{H-NMR}$ (500 MHz, $\text{DMSO-}d_6$): δ 10.65 (s, br 1H, NH), 10.55 (s, 1H, OH), 7.26–7.32 (m, 2H, H_{Bz}), 7.16–7.22 (m, 3H, H_{Bz}), 6.49 (s, br, 2H, NH_2), 3.64 (t, 2H, $J = 7.5$ Hz, CH_2), 2.57 (t, 2H, $J = 7.5$ Hz, CH_2), 1.91 (quin, 2H, $J = 7.5$ Hz, CH_2). $^{13}\text{C-NMR}$ (500 MHz, $\text{DMSO-}d_6$): δ 154.48 (C2), 152.86 (C4), 146.62 (C6), 141.71 (C8), 140.81 (C_{Bz}), 131.10 (CH_{Bz}), 131.06 (CH_{Bz}), 128.78 (CH_{Bz}), 128.70 (CH_{Bz}), 126.30 (CH_{Bz}), 98.42 (C5), 33.21 (NCH_2), 30.37 (CH_2), 29.06 (CH_2). m/z (FTMS + ESI) = Found $[\text{M}+\text{H}]^+$ ($\text{C}_{14}\text{H}_{15}\text{N}_5\text{O}_2$) 286.1301 requires 285.3070.

6-(methylthio)-9H-purine (15a)

According to the general alkylation method 3 with 6-mercaptapurine monohydrate (200 mg, 1.18 mmol), DMF (3 ml), DBU (0.18 ml, 1.18 mmol) and iodomethane (0.15 ml, 2.35 mmol) for 3 h. The product extracted with chloroform, and purified by column chromatography with $\text{CH}_2\text{Cl}_2/\text{MeOH}$ 95:5 as an eluent to afford a white solid of yield 110 mg, 56%. $^1\text{H-NMR}$ (500 MHz, $\text{DMSO-}d_6$): δ 13.51 (s, br, 1H, NH), 8.71 (s, 1H, H2), 8.44 (s, 1H, H8), 2.67 (s, 3H, CH_3). $^{13}\text{C-NMR}$ (500 MHz, $\text{DMSO-}d_6$): δ 151.99 (C2), 143.63 (C8), 11.66 (CH_3). m/z (FTMS + ESI) = Found $[\text{M}+\text{H}]^+$ ($\text{C}_6\text{H}_6\text{N}_4\text{S}$) 167.0383 requires 166.2020.

6-(ethylthio)-7H-purine (15b)

According to the general alkylation method 3 with 6-mercaptapurine monohydrate (200 mg, 1.18 mmol), DMF (3 ml), DBU (0.18 ml, 1.18 mmol) and bromoethane (0.18 ml, 2.35 mmol) for 3 h. The product extracted with chloroform, and purified by column chromatography with $\text{CH}_2\text{Cl}_2/\text{MeOH}$ 95:5 as an eluent to afford a white solid of yield 170 mg, 80%. $^1\text{H-NMR}$ (500 MHz, $\text{DMSO-}d_6$): δ 13.51 (s, br, 1H, NH), 8.70 (s, 1H, H2), 8.44 (s, 1H, H8), 3.34 (q, 2H, $J = 7.0$ Hz, SCH_2), 1.37 (t, 3H, $J = 7.0$ Hz, CH_3). $^{13}\text{C-NMR}$ (500 MHz, $\text{DMSO-}d_6$): δ 151.96 (C2),

147.82 (C8), 22.87 (SCH_2), 15.42 (CH_3). m/z (FTMS + ESI) = Found $[\text{M}+\text{H}]^+$ ($\text{C}_7\text{H}_8\text{N}_4\text{S}$) 181.0541 requires 180.2290.

6-(propylthio)-7H-purine (15c)

According to the general alkylation method 3 with 6-mercaptapurine monohydrate (200 mg, 1.18 mmol), DMF (3 ml), DBU (0.18 ml, 1.18 mmol) and 1-bromopropane (0.21 ml, 2.35 mmol) for 3 h. The product extracted with chloroform, and purified by column chromatography with $\text{CH}_2\text{Cl}_2/\text{MeOH}$ 95:5 as an eluent to afford a white solid of yield 140 mg, 61%. $^1\text{H-NMR}$ (500 MHz, $\text{DMSO-}d_6$): δ 13.50 (s, br, 1H, NH), 8.69 (s, 1H, H2), 8.43 (s, 1H, H8), 3.33 (t, 2H, $J = 7.5$ Hz, SCH_2), 1.73 (sext, 2H, $J = 7.5$ Hz, CH_2), 1.01 (t, 3H, $J = 7.5$ Hz, CH_3). $^{13}\text{C-NMR}$ (500 MHz, $\text{DMSO-}d_6$): δ 151.93 (C2), 143.27 (C8), 30.15 (SCH_2), 23.10 (CH_2), 13.70 (CH_3). m/z (FTMS + ESI) = Found $[\text{M}+\text{H}]^+$ ($\text{C}_8\text{H}_{10}\text{N}_4\text{S}$) 195.0696 requires 194.2560.

6-(isobutylthio)-7H-purine (15d)

According to the general alkylation method 3 with 6-mercaptapurine monohydrate (200 mg, 1.18 mmol), DMF (3 ml), DBU (0.18 ml, 1.18 mmol) and 1-bromo-2-methylpropane (0.26 ml, 2.35 mmol) for 3 h. The product extracted with chloroform, and purified by column chromatography with $\text{CH}_2\text{Cl}_2/\text{MeOH}$ 95:5 as an eluent to afford a white solid of yield 90 mg, 37%. $^1\text{H-NMR}$ (500 MHz, $\text{DMSO-}d_6$): δ 13.50 (s, br, 1H, NH), 8.68 (s, 1H, H2), 8.44 (s, 1H, H8), 3.29 (d, 2H, $J = 6.5$ Hz, SCH_2), 1.97 (sep, 1H, $J_1 = 6.5$ Hz, $J_2 = 7.0$ Hz, CH), 1.02 (d, 6H, $J = 6.5$ Hz, $2 \times \text{CH}_3$). $^{13}\text{C-NMR}$ (500 MHz, $\text{DMSO-}d_6$): δ 151.86 (C2), 143.68 (C8), 36.38 (SCH_2), 28.68 (CH_2), 22.09 ($2 \times \text{CH}_3$). m/z (FTMS + ESI) = Found $[\text{M}+\text{H}]^+$ ($\text{C}_9\text{H}_{12}\text{N}_4\text{S}$) 209.1011 requires 208.2830.

6-(benzylthio)-9H-purine (15e)

According to the general alkylation method 3 with 6-mercaptapurine monohydrate (200 mg, 1.18 mmol), DMF (3 ml), DBU (0.18 ml, 1.18 mmol) and benzyl bromide (0.28 ml, 2.35 mmol) for 3 h. The product extracted with chloroform, and purified by column chromatography with $\text{CH}_2\text{Cl}_2/\text{MeOH}$ 95:5 as an eluent to afford a white solid of yield 140 mg, 49%. $^1\text{H-NMR}$ (500 MHz, $\text{DMSO-}d_6$): δ 13.55 (s, br, 1H, NH), 8.75 (s, 1H, H2), 8.46 (s, 1H, H8), 7.46 (d, 2H, $J = 7.5$ Hz, H_{Bz}), 7.32 (t, 2H, $J = 7.0$ Hz, H_{Bz}), 7.25 (t, 1H, $J_1 = 7.0$ Hz, $J_2 = 7.5$ Hz, H_{Bz}), 4.66 (s, 2H, SCH_2). $^{13}\text{C-NMR}$ (500 MHz, $\text{DMSO-}d_6$): δ 151.92 (C2), 143.97 (C8), 138.35 (C_{Bz}), 129.46 (CH_{Bz}), 128.96 (CH_{Bz}), 127.64 (CH_{Bz}), 32.10 (SCH_2). m/z (FTMS + ESI) = Found $[\text{M}+\text{H}]^+$ ($\text{C}_{12}\text{H}_{10}\text{N}_4\text{S}$) 243.0716 requires 242.3000.

6-(phenethylthio)-9H-purine (15f)

According to the general alkylation method 3 with 6-mercaptapurine monohydrate (200 mg, 1.18 mmol), DMF (3 ml), DBU (0.18 ml, 1.18 mmol) and 2-bromoethylbenzene (0.32 ml, 2.35 mmol) for 3 h. The product extracted with chloroform, and purified by column chromatography with CH₂Cl₂/MeOH 95:5 as an eluent to afford a white solid of yield 160 mg, 53%. ¹H-NMR (500 MHz, DMSO-*d*₆): δ 13.52 (s, br, 1H, NH), 8.73 (s, 1H, H2), 8.45 (s, 1H, H8), 7.31–7.32 (m, 4H, H_{Bz}), 7.21–7.25 (m, 1H, H_{Bz}), 3.61 (t, 2H, *J* = 7.0 Hz, CH₂), 3.03 (t, 2H, *J* = 7.0 Hz, CH₂). ¹³C-NMR (500 MHz, DMSO-*d*₆): δ 152.01 (C2), 143.33 (C8), 140.58 (C_{Bz}), 129.07 (CH_{Bz}), 128.85 (CH_{Bz}), 126.82 (CH_{Bz}), 35.61 (SCH₂), 29.72 (CH₂). *m/z* (FTMS + ESI) = Found [M+H]⁺ (C₁₃H₁₂N₄S) 257.0850 requires 256.3270.

6-((3-phenylpropyl)thio)-9H-purine (15g)

According to the general alkylation method 3 with 6-mercaptapurine monohydrate (200 mg, 1.18 mmol), DMF (3 ml), DBU (0.18 ml, 1.18 mmol) and 1-bromo-3-phenylpropane (0.37 ml, 2.35 mmol) for 3 h. The product extracted with chloroform, and purified by column chromatography with CH₂Cl₂/MeOH 95:5 as an eluent to afford a white solid of yield 200 mg, 63%. ¹H-NMR (500 MHz, DMSO-*d*₆): δ 13.52 (s, br, 1H, NH), 8.68 (s, 1H, H2), 8.45 (s, 1H, H8), 7.28–7.31 (m, 2H, H_{Ph}), 7.17–7.24 (m, 3H, H_{Ph}), 3.35 (t, 2H, *J* = 7.3 Hz, CH₂), 2.76 (t, 2H, *J* = 7.5 Hz, CH₂), 2.03 (quin, 2H, *J*₁ = 7.3, *J*₂ = 7.5 Hz, CH₂). ¹³C-NMR (500 MHz, DMSO-*d*₆): δ 151.94 (C2), 141.61 (C_{Ph}), 128.82 (CH_{Ph}), 126.36 (CH_{Ph}), 39.48 (SCH₂), 31.28 (CH₂), 27.87 (CH₂). *m/z* (FTMS + ESI) = Found [M+H]⁺ (C₁₄H₁₄N₄S) 271.1011 requires 270.3540.

2,6-bis(methylthio)pyrimidine-4,5-diamine (16a)

According to the general alkylation method 1 with 4,5-diamino-2,6-dimercaptopyrimidine (200 mg, 1.0 mmol), potassium carbonate (150 mg, 1.1 mmol) and iodomethane (0.07 ml, 1.2 mmol) for 3 h. The product was purified by column chromatography with CH₂Cl₂/MeOH 95:5 as an eluent to afford an off-white solid of yield 112 mg, 49%. ¹H-NMR (500 MHz, MeOD): δ 2.57 (s, 3H, SCH₃), 2.50 (s, 3H, SCH₃). ¹³C-NMR (500 MHz, MeOD): δ 159.25 (C2), 152.82 (C6), 149.96 (C4), 118.09 (C5), 12.75 (2xSCH₃), 11.55 (SCH₃). *m/z* (FTMS + ESI) = Found [M+H]⁺ (C₆H₁₀N₄S₂) 203.0419 requires 202.2940.

2,6-bis(ethylthio)pyrimidine-4,5-diamine (16b)

According to the general alkylation method 1 with 4,5-diamino-2,6-dimercaptopyrimidine (100 mg, 0.57 mmol),

potassium carbonate (150 mg, 1.1 mmol) and bromoethane (0.09 ml, 1.2 mmol) for 3 h. The product was purified by column chromatography with CH₂Cl₂/MeOH 95:5 as an eluent to afford an off-white solid of yield 99 mg, 76%. ¹H-NMR (500 MHz, MeOD): δ 3.20 (q, 2H, *J* = 7.0 Hz, SCH₂), 3.08 (q, 2H, *J* = 7.0 Hz, SCH₂), 1.37 (t, 3H, *J* = 7.0 Hz, CH₃), 1.36 (t, 3H, *J* = 7.5 Hz, CH₃). ¹³C-NMR (500 MHz, MeOD): δ 158.58 (C2), 152.99 (C6), 148.97 (C4), 118.60 (C5), 24.52 (SCH₂), 23.86 (SCH₂), 14.49 (CH₃), 14.18 (CH₃). *m/z* (FTMS + ESI) = Found [M+H]⁺ (C₈H₁₄N₄S₂) 230.9 requires 230.3.

2,6-bis(propylthio)pyrimidine-4,5-diamine (16c)

According to the general alkylation method 1 with 4,5-diamino-2,6-dimercaptopyrimidine (200 mg, 1.0 mmol), potassium carbonate (150 mg, 1.1 mmol) and 1-bromopropane (0.06 ml, 1.2 mmol) for 3 h. The product was purified by column chromatography with CH₂Cl₂/MeOH 95:5 as an eluent to afford an off-white solid of yield 180 mg, 63%. ¹H-NMR (500 MHz, MeOD): δ 3.18 (t, 2H, *J* = 7.5 Hz, SCH₂), 3.06 (t, 2H, *J* = 7.5 Hz, SCH₂), 1.73 (sext, 4H, *J* = 7.5 Hz, CH₂), 1.05 (td, 6H, *J*₁ = 7.5 Hz, *J*₂ = 1.0 Hz, CH₃). ¹³C-NMR (500 MHz, MeOD): δ 158.59 (C2), 152.92 (C6), 149.11 (C4), 118.49 (C5), 32.31 (SCH₂), 31.40 (SCH₂), 23.33 (2xCH₂), 23.04 (2xCH₂), 12.44 (2xCH₃), 12.31 (CH₃). *m/z* (FTMS + ESI) = Found [M+H]⁺ (C₁₀H₁₈N₄S₂) 259.1045 requires 258.4020.

2,6-bis(isobutylthio)pyrimidine-4,5-diamine (16d)

According to the general alkylation method 1 with 4,5-diamino-2,6-dimercaptopyrimidine (100 mg, 0.57 mmol), potassium carbonate (150 mg, 1.1 mmol) and 1-bromo-2-methylpropane (0.13 ml, 1.2 mmol) for 3 h. The product was purified by column chromatography with CH₂Cl₂/MeOH 95:5 as an eluent to afford a light brown solid of yield 90 mg, 50%. ¹H-NMR (500 MHz, MeOD): δ 3.14 (d, 2H, *J* = 6.5 Hz, SCH₂), 3.01 (d, 2H, *J* = 7.0 Hz, SCH₂), 1.89–2.00 (m, 2H, CH), 1.06 (d, 3H, *J* = 2.0 Hz, CH₃), 1.05 (d, 3H, *J* = 2.5, CH₃). ¹³C-NMR (500 MHz, MeOD): δ 158.57 (C2), 152.87 (C6), 149.11 (C4), 118.43 (C5), 38.94 (SCH₂), 37.91 (SCH₂), 28.81 (CH), 28.47 (CH), 20.93 (4xCH₃). *m/z* (FTMS + ESI) = Found [M+H]⁺ (C₁₂H₂₂N₄S₂) 287.0228 requires 286.4560.

2,6-bis(benzylthio)pyrimidine-4,5-diamine (16e)

According to the general alkylation method 1 with 4,5-diamino-2,6-dimercaptopyrimidine (200 mg, 1.0 mmol), potassium carbonate (150 mg, 1.1 mmol) and benzyl bromide (0.14 ml, 1.2 mmol) for 3 h. The product was purified by column chromatography with CH₂Cl₂/MeOH 95:5 as an

eluent to afford an off-white solid of yield 190 mg, 50%. ¹H-NMR (500 MHz, MeOD): δ 7.37–7.39 (m, 2H, H_{Bz}), 7.19–7.31 (m, 10H, H_{Bz}), 4.38 (s, 2H, SCH₂), 4.34 (s, 2H, SCH₂). ¹³C-NMR (500 MHz, MeOD): δ 158.08 (C2), 153.16 (C6), 147.77 (C4), 138.50 (C_{Bz}), 138.25 (C_{Bz}), 128.02 (CH_{Bz}), 128.36 (CH_{Bz}), 128.02 (CH_{Bz}), 127.97 (CH_{Bz}), 126.66 (CH_{Bz}), 126.48 (CH_{Bz}), 119.16 (C5), 34.66 (SCH₂), 33.89 (SCH₂). *m/z* (FTMS + ESI) = Found [M + H]⁺ (C₁₈H₁₈N₄S₂) 355.1015 requires 354.4900.

2,6-bis(phenethylthio)pyrimidine-4,5-diamine (16f)

According to the general alkylation method 1 with 4,5-diamino-2,6-dimercaptopyrimidine (200 mg, 1.0 mmol), potassium carbonate (150 mg, 1.1 mmol) and 2-bromoethyl benzene (0.16 ml, 1.2 mmol) for 5 h. The product was purified by column chromatography with CH₂Cl₂/MeOH 95:5 as an eluent to afford an off-white solid of yield 260 mg, 64%. ¹H-NMR (500 MHz, MeOD): δ 7.15–7.26 (m, 10H, H_{Bz}), 3.45 (t, 2H, *J* = 7.5 Hz, SCH₂), 3.34 (t, 2H, *J* = 7.5 Hz, SCH₂), 2.96 (dt, 4H, *J*₁ = 7.5 Hz, *J*₂ = 3.5 Hz, 2xCH₂). ¹³C-NMR (500 MHz, MeOD): δ 158.39 (C2), 153.07 (C6), 149.11 (C4), 140.64 (C_{Bz}), 140.23 (C_{Bz}), 128.24 (CH_{Bz}), 128.21 (CH_{Bz}), 128.03 (CH_{Bz}), 125.95 (CH_{Bz}), 125.83 (CH_{Bz}), 118.95 (C5), 36.18 (CH₂), 35.98 (CH₂), 31.73 (SCH₂), 30.93 (SCH₂). *m/z* (FTMS + ESI) = Found [M + H]⁺ (C₂₀H₂₂N₄S₂) 383.1298 requires 382.5440.

2,6-bis((3-phenylpropyl)thio)pyrimidine-4,5-diamine (16g)

According to the general alkylation method 1 with 4,5-diamino-2,6-dimercaptopyrimidine (169 mg, 1.0 mmol), potassium carbonate (128 mg, 1.1 mmol) and 1-bromo-3-phenylpropane (0.15 ml, 1.2 mmol) for 5 h. The product was purified by column chromatography with CH₂Cl₂/MeOH 95:5 as an eluent to afford an off-white solid of yield 260 mg, 60%. ¹H-NMR (500 MHz, MeOD): δ 7.25 (dd, 4H, *J*₁ = 15.5 Hz, *J*₂ = 8.0 Hz, H_{Ph}), 7.15 (m, 6H, H_{Ph}), 3.14 (dd, 2H, *J*₁ = 13 Hz, *J*₂ = 7.0 Hz, SCH₂), 3.03 (t, 2H, *J* = 7.0 Hz, SCH₂), 2.72 (t, 4H, *J* = 7.0 Hz, CH₂), 1.92–2.00 (m, 4H, 2xCH₂). ¹³C-NMR (500 MHz, MeOD): δ 158.43 (C2), 152.96 (C6), 148.84 (C4), 141.53 (C_{Ph}), 141.33 (C_{Ph}), 128.12 (CH_{Ph}), 128.11 (CH_{Ph}), 128.03 (CH_{Ph}), 128.01 (CH_{Ph}), 125.54 (CH_{Ph}), 125.50 (CH_{Ph}), 118.72 (C5), 34.49 (C_{Ph}), 34.32 (CH₂), 31.59 (CH₂), 31.37 (SCH₂), 29.78 (SCH₂), 28.95 (SCH₂). *m/z* (FTMS + ESI) = Found [M + H]⁺ (C₂₂H₂₆N₄S₂) 411.2652 requires 410.5980.

Biological evaluation

MTT assay

(Mosmann 1983) Breast cancer cell lines MDA-MB-231 and MDA-MB-436 were maintained in Delbecco's

Modified Eagle's Media (DMEM) supplemented with 10% FCS. Human microvascular endothelial (HMVECs) were maintained in microvascular endothelial cell basal medium 131 with growth supplement (Gibco). MCF10A cells were maintained in mammary epithelial cell growth medium (Lonza) optimized for the growth of mammary epithelial cells in a serum-free environment. All cells were incubated at 37 °C in 5% CO₂. Cells were seeded in a 96-well plate at a density of 5 × 10³ cells/ml and incubated for 24 h at 37 °C and 5% CO₂. The cells were then treated with different concentrations of the test compounds and controls and incubated for 72 h. After this period, 20 μL of sterile MTT solution in PBS (5 mg/mL) was added to each well. The plates were then incubated for 5 h at 37 °C and 5% CO₂. Following this, 100 μL of acidified isopropanol was added (0.02% 2M HCl) and the mixture was allowed to stand until the formed formazan crystals had dissolved. The absorbance was measured at 570 nm (BioTeK), and the cell viability was expressed as a percentage of the absorbance of non-treated cells. The experiments were performed in three independent repeats, and the results were expressed as the mean ± the standard error of the mean (SEM).

Cytotoxicity assay

(Essen Bioscience 2017) MDA-MB-231, MDA-MB-436, HMVECs and MCF10A cells were seeded (100 μL per well) at a cell density of 5000 cells/well into a 96-well plate and incubated at 37 °C in 5% CO₂ within the IncuCyte ZOOM® system for 24 h. Contrast images were captured every 2 h and analysed using an integrated confluence algorithm. The test compounds and controls were prepared in the media containing the IncuCyte™ Cytotox Reagent at 3x the final concentration, then 50 μL of this solution was added to each well to obtain a dilution of 1:3 with a final assay volume of 150 μL (final assay concentration of Cytotox Reagent 250 nM). Images of the plate were captured at 10x objective, two images per well with phase and fluorescence scanning every 2 h until completion of the assay (72 h). The data were analysed using integrated software.

PathHunter™ cell-based CRYAB/VEGF₁₆₅ interaction assay

The cells were maintained in a PathHunter Assaycomplete™ culture media and incubated at 37 °C and 5% CO₂ until confluent. The U2OS cells were detached with Assaycomplete™ cell detachment reagent, suspended in Assaycomplete™ cell plating reagent and counted. In total, 20 μL of the cell suspension was transferred to each well of a 384-well white-walled, clear bottom plate at the indicated cell densities (5000, 10000, 20000 cells/ml).

The seeded cells were incubated for 24 h at 37 °C and 5% CO₂, 5 µL of the test compounds (10 µM) dissolved in the vehicle (2% DMSO) were added to the appropriate wells and incubated at room temperature for 90 min. After incubating, 25 µL per well of PathHunter Detection Reagents were added to the plates, incubated for 60 min at room temperature in the dark and the plate read using the POLARstar Omega luminescence reader.

ELISA assay

VEGF₁₆₅ secreted by MDA-MB-231 cells were assayed using Quantio® ELISA assay kit (R&D Systems). The assay was performed according to the manufacturers' instructions. MDA-MB-231 cells were grown in a T25 flask at 37 °C and 5% CO₂ until 80% confluence. The cells were then treated with the test compounds dissolved in DMSO (0.1%). The cell supernatant was harvested by centrifugation at 2000 × g for 15 min at 6, 12 and 24 h. VEGF₁₆₅ concentrations were measured in triplicate in each sample. The results are expressed as VEGF₁₆₅ pg/ml for at least three separate experiments.

Molecular modelling

All molecular modelling studies were performed with Molecular Operating Environment (MOE) 2015.10 modelling software. The crystal structure of the ACD domain of CRYAB was obtained from the Protein Data Bank (PDB code: 2KLR). Hydrogen atoms were added to the crystal structure minimised with MOE until a gradient of 0.05 Kcal mol⁻¹ Å⁻¹ was reached, using the MMFF94x forcefield. The partial charges were automatically calculated. To simplify calculations and analysis within this hydrophobic active site, no water molecules were considered. The docking site was defined by selecting the important amino acid residues (Tyr122, Arg 123 and Arg 149) and extending to 4.5 Å to include other β7 and β9 amino acid residues. Ligand docking was performed using MOE default settings. After docking, all docked molecules were visually inspected.

Results and discussion

Design of novel analogues and synthetic chemistry

We began our synthetic studies around a dithiopurine-8-one heterocyclic core, proposing the introduction of substituents to improve lipophilicity and enhance cellular penetration. We decided to explore alkylation chemistry to derivatise the core dithiopurine-8-one heterocyclic structure particularly at the sulphur and/or the N7/N9 positions, as well as introducing functional flexibility at position C8. Figure 2 shows the proposed structural changes and exploratory chemistry leading to five small series of new molecules for in vitro anticancer evaluation.

There is clear evidence in the literature that reaction conditions play a crucial role in determining the selectivity of alkylation of purines and pyrimidines. Therefore, various conditions reported in the literature were examined to ascertain the optimal reactions conditions required to obtain selective alkylation at the appropriate positions of the purinone core (Pathak et al. 2004; Cheng and Robins 1958; Robins 1958; Biagi et al. 1996; Corder et al. 2013; Johnston et al. 1958; Robins 1957). Scheme 1 outlines the synthetic route employed in the synthesis of Series 1 analogues **4a–g**, characterised by derivatisation of the sulphur groups at positions 2 and 6 with various alkyl groups. The purine core structure **2** was prepared via a thermal cyclisation reaction between the commercially available pyrimidine **1** and urea (Levin et al. 1960). As suggested in the literature, it was expected that under alkaline conditions, alkylation of compound **2** would selectively produce the exclusively S-alkylated product (Joule et al. 1995; Montgomery et al. 1966). In addition, it has been reported that low reaction temperatures favour S- over N-alkylation. However, it was noted that when using K₂CO₃ or KOH as a base, the tri-substituted product (**3**) was produced regardless of the stoichiometry of the reagents. The best conditions found to facilitate selective S-alkylation to provide the double alkylation products (**4a–g**) involved the non-nucleophilic base, 1,8-diazabicyclo[5.4.0]undec-7-ene (DBU) in DMF (Biagi et al. 1996), in yields of 29–74% following purification by column chromatography.

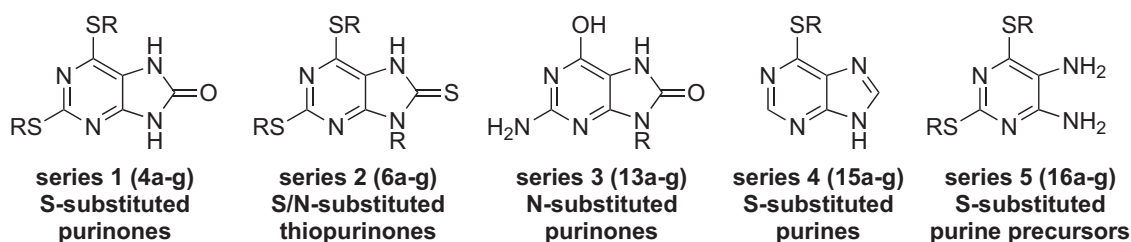
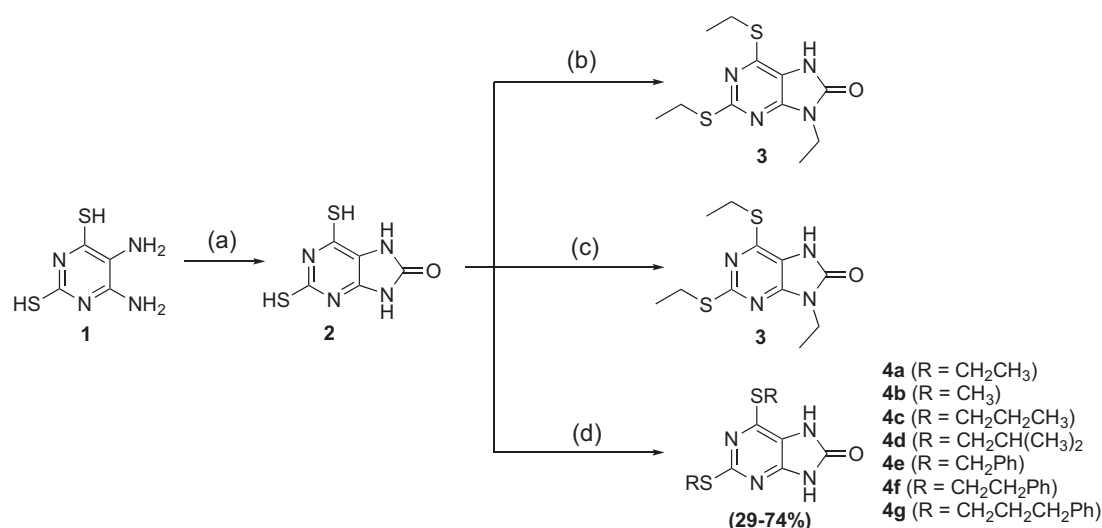
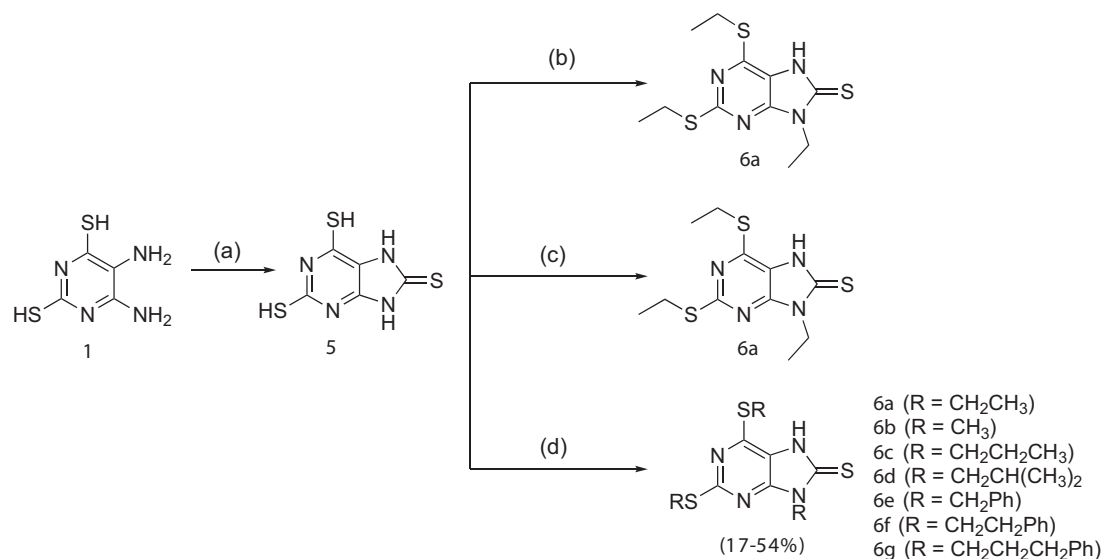


Fig. 2 Target molecule series derived from the dithiopurine-8-one core structure



Scheme 1 Synthesis of Series 1 analogues. Reagents and conditions: **a** urea, 180–195 °C, 20 min; **b** CH₂CH₃Br, K₂CO₃, DMF, r.t., 2.5 h; **c** CH₂CH₃Br, 1 M KOH, r.t., 2.5 h; **d** R-Br/I, DBU, DMF, r.t., 2.5 h



Scheme 2 Synthesis of Series 2 analogues. Reagents and conditions: **a** thiourea, 180–195 °C, 20 min; **b** CH₂CH₃Br, K₂CO₃, DMF, r.t., 2.5 h; **c** CH₂CH₃Br, 1 M KOH, r.t., 2.5 h; **d** R-Br/I, DBU, DMF, r.t., 2.5 h

The synthetic route employed in the synthesis of Series 2 analogues **6a–g** is outlined in Scheme 2. A thermal cyclisation reaction between pyrimidine (**1**) and thiourea resulted in the 8-thiopyrimidine (**5**), which was followed by alkylation reactions with various alkyl halides as described in Scheme 1. Under all the investigated reaction conditions, the products of the alkylation reactions were the tri-substituted purines similar to the products obtained under the previously described alkaline conditions (K₂CO₃ or KOH), in low-to-moderate yields of 17–54% (Scheme 1). The acidity of the thiopyrimidine NH group adjacent to the

pyrimidine N3-atom provides a rationale for alkylation at the N9-position under basic conditions. Although tri-substituted purines have been reported in the literature, they are usually constructed from alkylated pyrimidines cyclised with alkoxides and not in a one-pot synthesis as we achieved (Yang et al. 2005; Villatoro et al. 2015; Ibrahim and Legraverend 2009).

Surprisingly in addition to the tri-substituted thiopyrimidine (**6b**), methylation of compound **5** also produced the tetra-substituted product **7** (Scheme 3). We postulated that methylation at position N7 is possible since the methyl

group is not affected by steric hindrance compared with the bulkier alkyl substituents.

Scheme 4 was employed to give access to selectively *N*-alkylated purines **13a–g** that were deemed necessary for SAR studies. Selective *N*-alkylation was readily achieved by a reaction between 2-amino-6-chloropurine **8** and various alkyl halides to afford compounds **9a–g/10a–g** as a mixture of regioisomers, with the *N*9-isomer (**9a–g**) being the major product as previously reported in the literature (Chhabra et al. 2013). Both isomers were successfully separated by silica gel chromatography and fully characterised by NMR. The ¹H NMR spectrum showed the alkyl peaks of the *N*7 product to be shifted downfield due to the deshielding effect of the bulky chloro group. The *N*9 products were then taken forward in a multi-step synthesis to give the desired *N*-alkylated purinones **13a–g** by introducing a keto-group at position 8. Compounds **9a–g** were hydrolysed in aqueous HCl to afford the intermediates **11a–g**, which were then brominated to afford the 8-bromopurine intermediates **12a–g** (Michael et al. 1993). Finally, the brominated purines were transformed to the desired 8-oxopurines **13a–g** through hydrolysis of the bromo group, in low to good yields (6–85%) (Verones et al. 2010).

Lastly, substituted 6-thiopurines **15a–g** and 2,6-dithiopyrimidines **16a–g**, which represent Series 4 and 5 analogues, respectively, were also synthesised from commercially available precursor compounds **14** and **31**, in

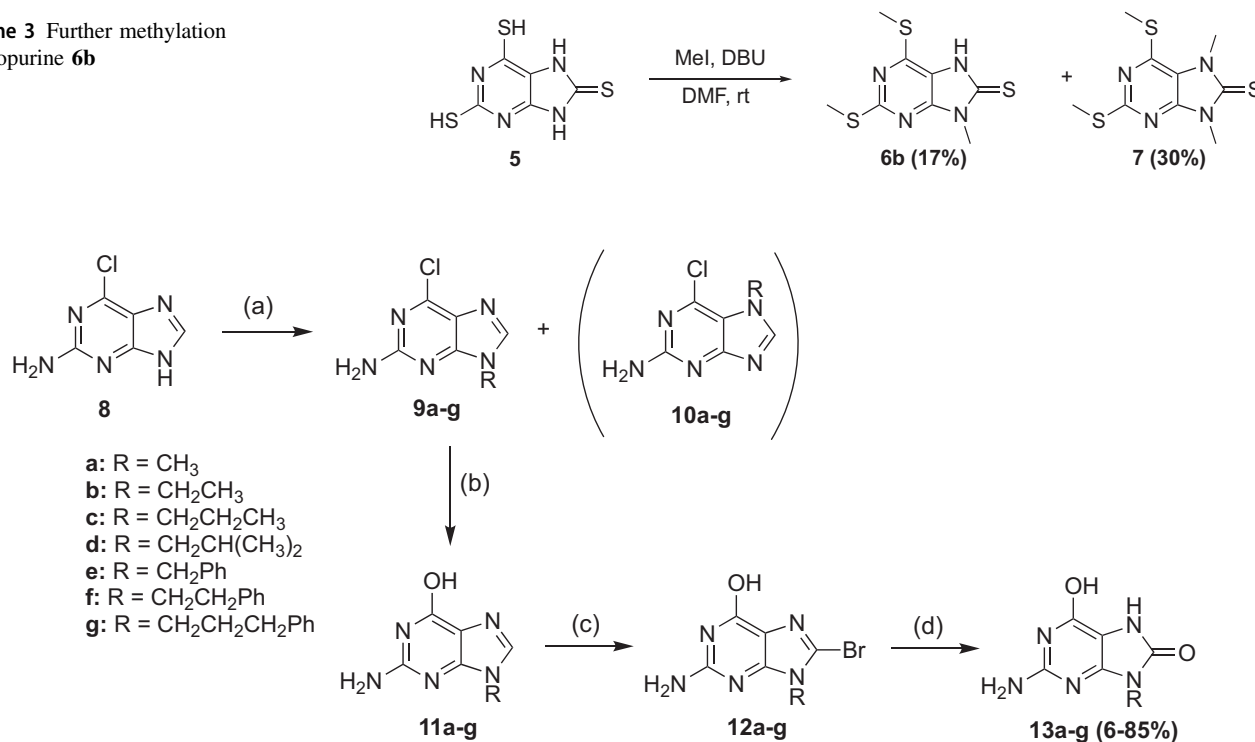
moderate-to-high yield (37–80%) following the previously described alkylation methods for further SAR studies (Scheme 5).

Biological evaluation—anti-proliferative activity

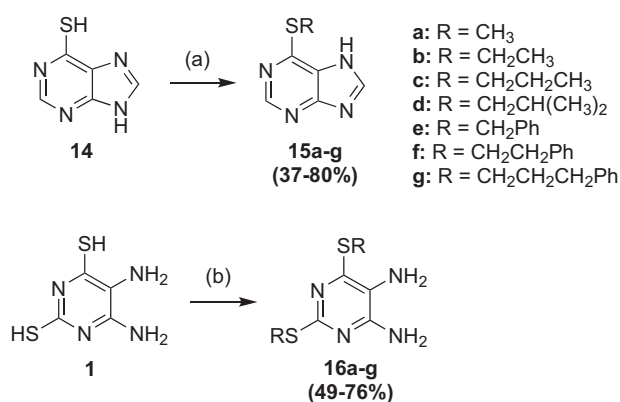
The analogues were tested for their *in vitro* inhibitory effect on the viability of the invasive TNBC cell lines MDA-MB-231 and MDA-MB-436, using the MTT endpoint assay (72 h). Additionally, endothelial cell lines, MCF10A and human microvascular endothelial (HMVEC-d) cell lines were used to assess the effects of the analogues on endothelial cells. Table 1 details the result of this *in vitro* screen expressed as IC₅₀ values from dose-response studies.

In general, several analogues from Series 1 (**4a–g**), Series 2 (**6a–g**) and Series 5 (**16a–g**) showed the most potent anti-proliferative effects, significantly reducing the viability of one or both TNBC cells with IC₅₀ values in the low micromolar range. It should be noted that active analogues were also generally more active as growth inhibitors in the endothelial cell lines HMVEC and MCF10A, perhaps not surprisingly for these early stage lipophilic drug candidates. The selectivity profiles between the different cell types certainly underscore the importance of carrying out more detailed toxicity studies in the future.

Scheme 3 Further methylation of thiopurine **6b**



Scheme 4 Synthesis of Series 3 analogues. Reagents and conditions: **a** RBr/I, K₂CO₃, DMF, r.t., 2.5 h; **b** 1 M HCl, reflux, 3 h; **c** Br₂, AcOH, 50–60 °C, 18 h; **d** CH₃COONa, AcOH/Ac₂O, reflux, 18 h



Scheme 5 Synthesis of Series 4 and 5 analogues. Reagents and conditions: **a** R-Br/I, DBU, DMF, r.t., 2.5 h; **b** RBr/I, K₂CO₃, DMF, r.t., 2.5 h

Notably, benzyl/phenethyl substituted purinone/thiopurinone analogues **4e**, **4f**, and **6e**, were the most potent in TNBC cell lines, suggesting that this group may be important for biological activity. Across all series, it was also evident that the chain length of the alkyl substituents has an influence on biological activity. For analogues with aliphatic substituents, it was observed that isobutyl > propyl > ethyl > methyl in terms of their anti-proliferative activity within cell lines examined. For example, ethyl substituted analogue **4a** showed IC₅₀ values of 97 and 100 μM against MDA-MB-231 and MDA-MB-436 cells, respectively, compared with the propyl substituted analogue **4c**, which showed an IC₅₀ value of 29 μM against both TNBC cell lines. However, for analogues with alkyl benzyl substituents, an increase in the chain length of the alkyl benzyl group appears to have a detrimental effect on biological activity. For example, compound **4f** with a phenethyl group showed an IC₅₀ value of 3–4 μM in TNBC cell lines, while increasing the chain length to a phenylpropyl group as seen for compound **4g** resulted in a complete loss of activity (IC₅₀ > 100 μM).

Overall, analogues from Series 3 and 4 showed no inhibitory effects against either TNBC cell line apart from compound **15f** (Series 4). This suggests that the substitution at positions 2 and 6 and the keto group at position-8 may contribute to the observed biological effect. As noted above, the most potent analogues across all series also showed potent growth inhibitory effects on the epithelial and endothelial cell lines MCF10A and HMVEC-d, respectively, without the desired selectivity for TNBC cell lines.

Cytotoxicity evaluation

Compounds that demonstrated the most potent inhibitory effect in the anti-proliferative assay (IC₅₀ ≤ 50 μM) were evaluated for their ability to induce cytotoxicity against the cell lines under investigation. The in vitro cytotoxicity assay

was performed using the cyanine nucleic acid dyes developed by Essen BioScience with their IncuCyte™ live-cell imaging system that enables real time detection of cell death. The cells were co-cultured with the IncuCyte™ Cytotox reagent, and test compounds **4c**, **4e–f**, **6d–e**, **15f** and **16d** were added at different concentrations over a period of 72 h. Images were captured every 2 h for the duration of the assay and the cytotoxicity effect was quantified in real-time with the integrated analysis software. Generally, all the tested compounds showed a significant increase in the cell death characteristics of a cytotoxicity effect compared with the no-drug control, with a few notable exceptions (Fig. 3). All the seven compounds induced a cytotoxic effect at a concentration of 100 μM against the TNBC cells, while cytotoxic effects were detected at a concentration of 50 μM against endothelial cells. These results appear to correlate with the observed anti-proliferative activity and thus, provided confidence for these analogues to undergo further evaluation, notably in our custom cell-based CRYAB/VEGF₁₆₅ interaction assay to probe their ability to disrupt this interaction.

PathHunter™ cell-based CRYAB/VEGF₁₆₅ interaction assay

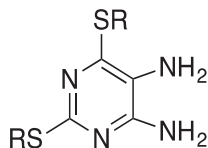
The PathHunter™ cell-based CRYAB/VEGF₁₆₅ interaction assay is a commercially available, custom cell-based assay designed by DiscoverX. The assay utilizes the enzyme fragment complementation (EFC) technology for studying protein–protein interactions. For the purposes of this research, the assay was designed to monitor the interaction between CRYAB and a cytosolically localised VEGF₁₆₅. The two candidate proteins were fused to complementation fragments of the β-galactosidase (β-Gal) enzyme. CRYAB was co-expressed with the larger sequence encoding the majority of enzyme, termed enzyme acceptor (EA), while VEGF₁₆₅ was fused to a small peptide epitope called Pro-link (PK). The two separate enzyme fragments are inactive; however, after the constructs were transduced into U2OS cells, the recombined active enzyme is generated as a result of CRYAB/VEGF₁₆₅ protein–protein interaction. The disruption of the CRYAB/VEGF₁₆₅ interaction was quantified by measuring the chemiluminescence signal produced as a consequence of the conversion of a non-luminescent substrate to a luminescent product by the active enzyme.

The U2OS cells were seeded at three cell densities (20,000, 10,000 and 5000 cells/well), allowed to adhere to the wells and challenged with different concentrations of the test compounds. Tunicamycin was used as a positive control for this assay because of its ability to elicit the unfolded protein response and thus inhibit angiogenesis (Banerjee et al. 2011). After 90-min incubation period, the non-luminescent substrates were introduced into the cells and

Table 1 Anti-proliferative activity of the synthesised analogues expressed as IC₅₀ ±SEM (three independent experiments)

Compound	R group	IC ₅₀ ±SEM (μM)			
		MDA-MB-231	MDA-MB-436	HMVEC	MCF10A
Series 1					
4a	CH ₂ CH ₃	97 ± 0.22	100	>100	>100
4b	CH ₃	>100	>100	>100	>100
4c	CH ₂ CH ₂ CH ₃	29 ± 1.3	29 ± 0.5	14 ± 0.07	12 ± 3.2
4d	CH ₂ CH(CH ₃) ₂	>100	>100	3 ± 0.16	1.5 ± 4.4
4e	CH ₂ Ar	17 ± 1.3	45 ± 1.1	4 ± 0.23	3 ± 0.12
4f	CH ₂ CH ₂ Ar	3 ± 0.35	4 ± 1.05	1 ± 0.23	9.6 ± 0.12
4g	CH ₂ CH ₂ CH ₂ Ar	>100	>100	2 ± 0.48	0.6 ± 0.08
Series 2					
6a	CH ₂ CH ₃	84 ± 1.1	>100	57 ± 1.5	19 ± 0.72
6b	CH ₃	80 ± 0.06	>100	45 ± 0.13	31 ± 0.14
6c	CH ₂ CH ₂ CH ₃	56 ± 0.89	99 ± 0.44	28 ± 0.71	3 ± 1.2
6d	CH ₂ CH(CH ₃) ₂	35 ± 0.11	36 ± 0.20	5 ± 0.14	1 ± 0.21
6e	CH ₂ Ar	5 ± 0.05	37 ± 0.08	3 ± 0.08	1.2 ± 0.17
6f	CH ₂ CH ₂ Ar	91 ± 0.15	>100	19 ± 0.19	1.3 ± 0.1
6g	CH ₂ CH ₂ CH ₂ Ar	>100	>100	>100	19 ± 0.06
Series 3					
13a	CH ₃	>100	>100	>100	>100
13b	CH ₂ CH ₃	>100	>100	>100	>100
13c	CH ₂ CH ₂ CH ₃	>100	>100	>100	>100
13d	CH ₂ CH(CH ₃) ₂	>100	>100	85 ± 0.10	>100
13e	CH ₂ Ar	>100	>100	69 ± 0.05	>100
13f	CH ₂ CH ₂ Ar	>100	>100	>100	80 ± 0.09
13g	CH ₂ CH ₂ CH ₂ Ar	>100	>100	>100	72 ± 0.04
Series 4					
15a	CH ₃	>100	>100	>100	>100
15b	CH ₂ CH ₃	>100	>100	>100	>100
15c	CH ₂ CH ₂ CH ₃	>100	>100	>100	>100
15d	CH ₂ CH(CH ₃) ₂	>100	>100	85 ± 0.10	>100
15e	CH ₂ Ar	>100	>100	69 ± 0.05	>100
15f	CH ₂ CH ₂ Ar	49 ± 0.06	>100	15 ± 0.05	83 ± 0.12
15g	CH ₂ CH ₂ CH ₂ Ar	>100	>100	49 ± 0.05	59 ± 0.37

Table 1 (continued)

Compound	R group	IC ₅₀ ±SEM (μM)			
		MDA-MB-231	MDA-MB-436	HMVEC	MCF10A
					
Series 5					
16a	CH ₃	>100	>100	30 ± 0.07	14 ± 0.07
16b	CH ₂ CH ₃	>100	>100	17 ± 0.08	2.1 ± 0.08
16c	CH ₂ CH ₂ CH ₃	61 ± 0.30	>100	34 ± 0.25	1.4 ± 0.11
16d	CH ₂ CH(CH ₃) ₂	21 ± 0.11	43 ± 0.11	33 ± 0.29	1.9 ± 0.16
16e	CH ₂ Ar	78 ± 0.07	>100	1 ± 0.06	0.2 ± 0.18
16f	CH ₂ CH ₂ Ar	>100	>100	10 ± 0.07	0.7 ± 0.24
16g	CH ₂ CH ₂ CH ₂ Ar	>100	>100	8 ± 0.07	0.6 ± 0.34

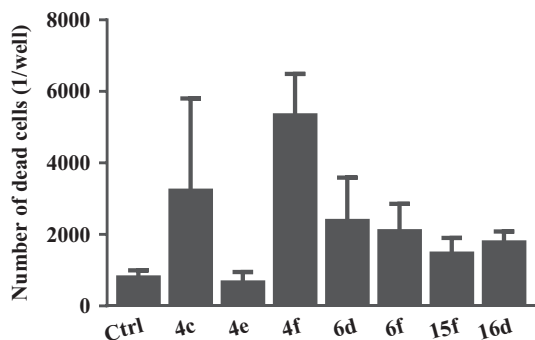
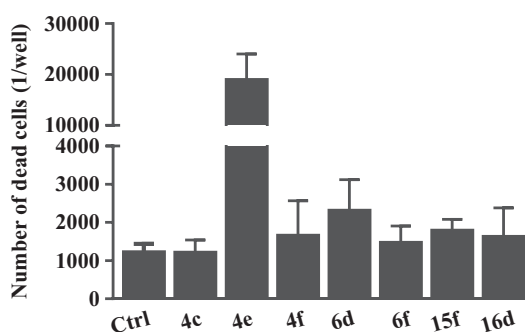
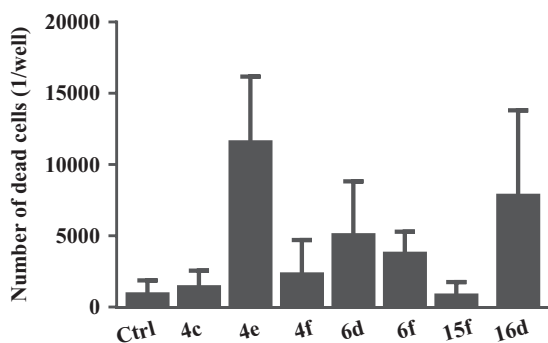
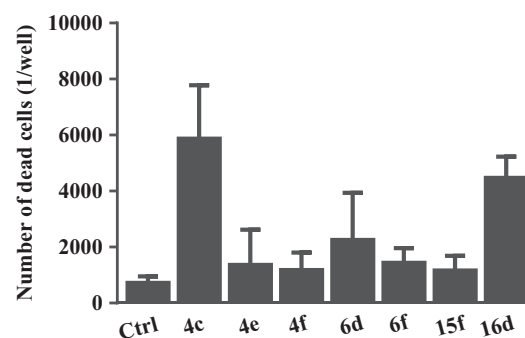
MDA-MB-231 (100 μM)

MDA-MB-436 (100 μM)

HMVEC-d (50 μM)

MCF10A (50 μM)


Fig. 3 Cytotoxic effect of selected analogues against TNBC and control cell lines. Data are expressed as mean ± standard error of the mean (SEM), $n = 3$

luminescent readings taken with a spectrophotometer after 60 min. All experiments were carried out in triplicate. The seven analogues that demonstrated inhibitory and cytotoxicity effects in previous experiments were selected for further evaluation in the cell-based CRYAB/VEGF₁₆₅

interaction assay. Out of the seven compounds, analogues **4e** and **4f** were found to significantly attenuate the chemiluminescence signal of U2OS cells at a density of 20,000 cells/well. No significant inhibition effect was observed for the remaining five analogues. The response (RLU) of the

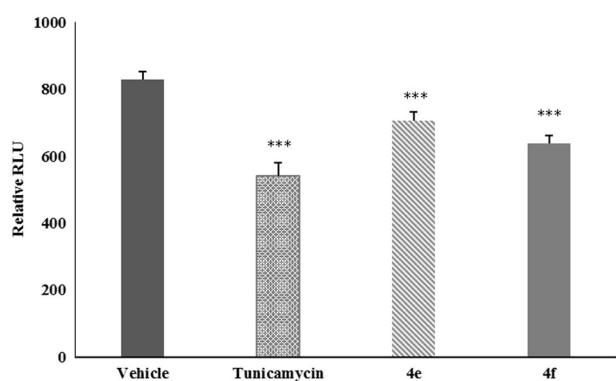


Fig. 4 Concentration-response curves of analogues **4e** and **4f** and controls in the PathHunter™ cell-based CRYAB/VEGF₁₆₅ interaction assay, indicating chemiluminescence quantification relative to the vehicle control; data are expressed as mean ± standard error of the mean (SEM), $n = 3$, *** $P < 0.001$

analogues at 10 μM and the controls are shown in Fig. 4. Both analogues and tunicamycin demonstrated a significant decrease in chemiluminescence signal in comparison with the vehicle control (DMSO). This inhibitory effect is indicative of the disruption of the interaction between CRYAB and VEGF₁₆₅.

VEGF₁₆₅ ELISA measurement

As previously discussed, one of the proposed mechanisms by which CRYAB promotes angiogenesis is by preventing the proteolytic degradation of misfolded or unfolded VEGF resulting in the upregulation of VEGF and maintenance of VEGF signalling (Ruan et al. 2011). Hence, we postulated that disrupting the interaction between CRYAB/VEGF would affect the levels of VEGF produced by breast cancer cells. The concentration of VEGF secreted by MDA-MB-231 cells was measured by the ELISA assay. MDA-MB-231 cells treated with 100 μM of compound **4e** showed a significant reduction in VEGF levels compared with the control. A concentration of 160 pg/ml of soluble VEGF was detected by the assay compared with the control (260 pg/ml), representing a 40% decrease in VEGF concentration (Fig. 5). No significant reduction was observed in cells treated with compound **4f**. This result supports our hypothesis that the disruption of the interaction between CRYAB/VEGF can lead to inhibition of VEGF production by breast tumour cells.

Molecular modelling studies

Previous work has reported sequence studies for the interaction of important regulatory proteins with CRYAB (Ghosh et al. 2007). Typical of most proteins of the Hsp family, the structure of CRYAB consists of an N-terminal region of ~65 amino acids, preceding a conserved

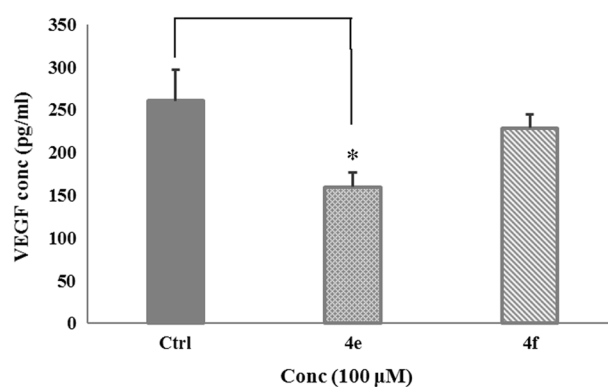


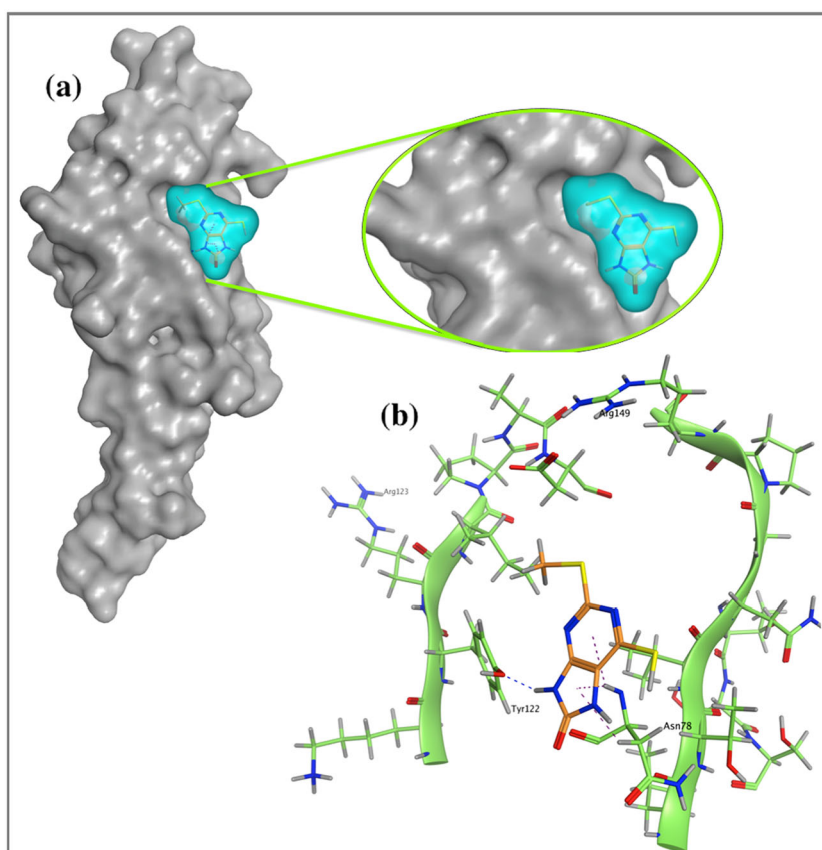
Fig. 5 ELISA measurement of VEGF₁₆₅ levels secreted by MDA-MB231 cells treated with 100 μM of compounds **4e** and **4f**. Data are expressed as mean ± standard error of the mean (SEM), $n = 3$; *** $P < 0.05$

α -crystallin domain (ACD) domain made up of 84 amino acids, and finally a C-terminal region composed of 26 amino acids. The ACD domain consists of eight β strands ($\beta 2$ to $\beta 9$) and helical sequences with strong interactions to regulatory proteins. The aforementioned sequence studies demonstrated that the β strands ($\beta 3$, $\beta 7$, $\beta 8$ and $\beta 9$) play a crucial role in the interactions between many growth factors and CRYAB, including VEGF₁₆₅. Additionally, an inhibitory competition study with decoy peptides corresponding to CRYAB and VEGF₁₆₅ confirmed the significance of $\beta 7$ and $\beta 9$ in the protein–protein interaction between CRYAB and VEGF₁₆₅ (Chen et al. 2014). Fortunately from the standpoint of computational drug design, a good crystal structure of the α -crystallin domain (ACD) of human CRYAB obtained from solid-state NMR, small angle X-ray scattering, and computational modelling studies has been published (PDB code: 2KLR) (Jehle et al. 2010).

On this basis, for docking studies a hydrophobic structural pocket was selected that was formed by discontinuous segments of $\beta 7$ and $\beta 9$ and containing the amino acids Try122/Arg123 ($\beta 7$) and Arg149 ($\beta 9$). In a series of docking simulations carried out with Molecular Operating Environment (MOE 2017), all the analogues and one additional monosubstituted purinone, 6-mercapto-2-(methylthio)purin-8-one, were docked into the selected structural pocket to probe their interaction with the target site.

Figure 6 shows the predicted binding pose of 6-mercapto-2-(methylthio)purin-8-one. The methylthio side group spatially occupies the structural pocket, albeit partially. Crucially, one of the nitrogen groups of the imidazolidine ring forms an H-bond with Tyr122. Moreover, there were other hydrophobic interactions between the purine ring and surrounding amino acids, including Asn78 of the $\beta 3$ strand. Comparatively, **4e** (Fig. 7) also retained the key interaction

Fig. 6 **a** Predicted binding mode of 6-mercapto-2-(methylthio)purin-8-one (orange) in selected docking site of CRYAB (grey), and **b** ligand interaction diagram (the compound is shown in orange while protein residues are in green)



with Tyr122 and an additional interaction with $\beta 7$ through a H-bond between a thiol group and Ile124. Compound **4f** (Fig. 8) interacts with $\beta 7$ through hydrophobic interaction between the purine core and Arg123. Furthermore, one of the nitrogen groups of the imidazolidine ring of both analogues forms a H-bond with Lys121 also of $\beta 7$. Finally, it was noted that the benzyl/phenethyl rings penetrates further and occupies more of the binding pocket compared with 6-mercapto-2-(methylthio)purin-8-one. Interestingly, even the aromatic ring of the benzyl/phenethyl groups does not fully occupy this pocket hence the presence of bulky substituents on the ring could promote better insertion, as well as new interactions that could improve on the biological activities of the analogues. Also noticeable is the fact that none of the compounds interact with $\beta 9$; this may be indicative of its distance (26 amino acids away) from $\beta 7$. Therefore, introducing bulky substituents to the aromatic ring could bring this group closer to $\beta 9$ and enhance the interaction between the molecules and CRYAB.

Discussion

The biological and docking studies have highlighted structural features that could be responsible for the observed

in vitro activities of the synthesised analogues and will inform future endeavours to design more efficacious CRYAB inhibitors. These observations are summarised below.

Effects of S-alkyl substituents

To improve on the lipophilicities of the purine core structure, various alkyl substituents were introduced to the thio- and/or nitrogen groups. It was observed that across all series, analogues with aromatic phenalkyl substituents demonstrated the most potent biological effects in the various assays. However, the chain length of the phenalkyl group was found to be a limiting factor, that is, an increase in chain length led to a decrease in activity. Furthermore, compounds **4e** and **4f**, with this benzyl/phenethyl functionality were able to disrupt the interaction between CRYAB/VEGF₁₆₅ in the protein–protein interaction assay. In addition, compound **4e** also decreased the levels of VEGF secreted by MDA-MB-231 cells. In our docking studies, the benzyl/phenethyl group was also found to form key interactions with the selected structural pocket on CRYAB confirming the significance of this group.

Fig. 7 **a** Predicted binding mode of compound **4e** (orange) in selected docking site of CRYAB (grey), **b** ligand interaction of compound **4e**

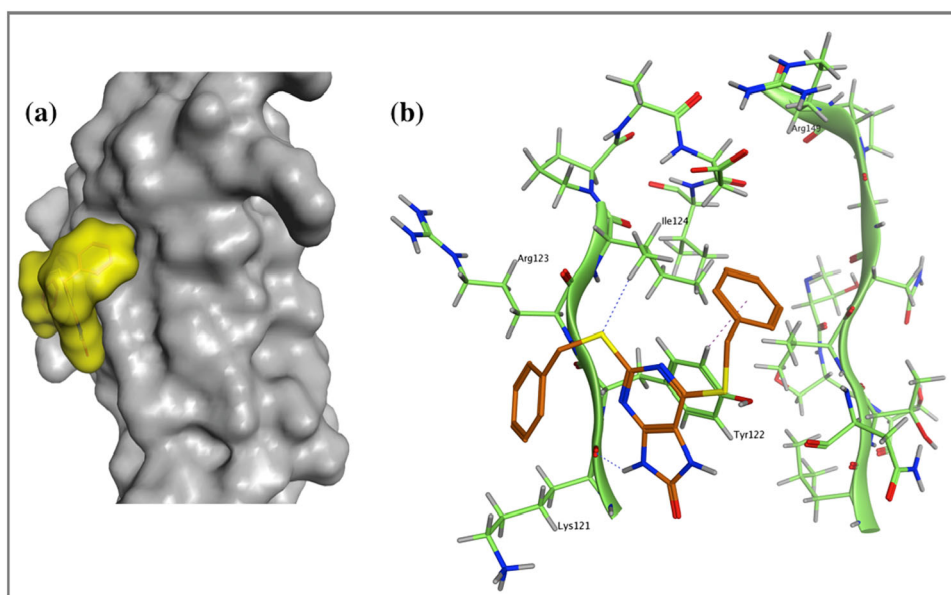
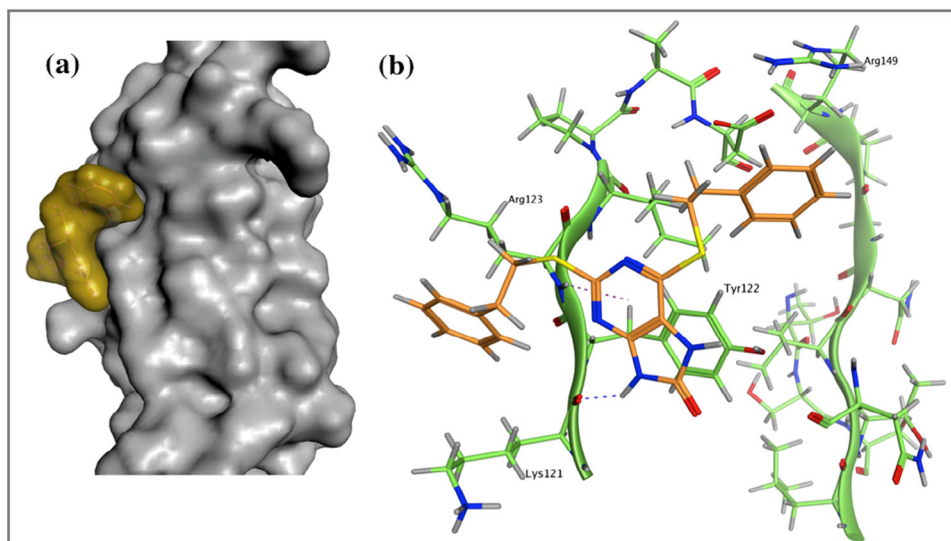


Fig. 8 **a** Predicted binding mode of compound **4f** (orange) in selected docking site of CRYAB (grey), **b** ligand interaction of **4f**



Effects of N-substitutions

No improvement in activity was observed for the series of analogues with *N*-substitutions (Series 3). Additionally, the docking studies showed no interactions between this substitution and CRYAB (data not shown).

Effects of removing the thio group at position-2

Removal of the thio-group at position-2 as seen with Series 3 and 4 analogues could be responsible for the loss of activity in both the various *in vitro* assays. Crucially, in the docking studies, it appears that this substitution interacts with the structural pocket of CRYAB indicating that this substitution contributes to the biological activities of the analogues.

Functional flexibility at position-8

As Series 4 analogues are effectively non-toxic against the control cell lines, it can be deduced that this substitution may contribute to the observed toxicity of the analogues. However, the toxicity effect may not be limited to this substituent but also the substituted thiol group at position-2, since analogues without this substitution (Series 3 and 4) showed little or no cytotoxic effect.

CRYAB confers protection against apoptosis induced by chemotherapeutic agents by inhibiting caspase-3 activation, sequestration of the anti-apoptotic protein Bcl-2 and prevention of Bcl-2 translocation into the mitochondria. In a study where breast epithelial carcinoma cells were treated with the anticancer agent vinblastine, the

phosphorylated form of CRYAB was found to inhibit apoptosis by interacting with Bcl-2, while non-phosphorylated CRYAB induced resistance against vinblastine (Launay et al. 2010). The silencing of CRYAB with antisense or RNAi molecules reversed this effect and sensitised tumour cells to chemotherapeutic and apoptotic agents (Lee et al. 2012). Angiogenesis, a segment of the metastatic cascade and the role of CRYAB as a facilitator of this phenomenon is of particular interest to our group. In the tumour microenvironment, CRYAB modulates angiogenesis through its effect on both cancer and endothelial cells. Studies have shown that CRYAB can prevent proteolytic degradation of VEGF by binding to and correcting unfolded/misfolded VEGF leading to preservation of intracrine VEGF signalling. Inhibition of CRYAB leads to a decrease in endogenous VEGF levels, providing clear evidence that targeting CRYAB may represent a novel approach to suppress angiogenesis. It should be noted that CRYAB is also expressed at high levels in the heart and cardiomyocytes, conferring protection against stress (such as an ischaemic event) by inhibiting apoptosis (Pereira et al. 2014; Gonçalves et al. 2016; Morrison et al. 2003). Therefore, direct inhibition of CRYAB could lead to unwanted cardiotoxicity. Consequently, we propose a novel strategy of targeting angiogenesis by disrupting the interaction between CRYAB and VEGF with small molecules that competitively bind to the interacting surface. This approach could produce a therapeutic effect while potentially avoiding the unwanted side effects associated with direct inhibition of CRYAB, and serve as a novel anti-angiogenic therapy in the treatment of TNBC.

Conclusions

Even though protein–protein interactions (PPI) are involved in many fundamental biological processes, designing small molecules to target PPI's has been deemed challenging due to the frequent occurrence of large and featureless protein interfaces. Over the last two decades, as our understanding of the interfaces have progressed, PPI's have become attractive molecular targets in drug development. Although the interfaces of PPI's are extensive, studies have shown that not all residues of these interfaces contribute towards the stability of the binding between target- and client proteins, but only the so-called “hotspots” (a number of conserved amino acid residues) are critical for interaction. Thus, most of these “hotspots” have become targets in the drug development process and the last few years have seen a number of small molecule PPI inhibitors enter clinical trials (White et al. 2008; Arkin et al. 2014).

Following this trend, we propose a novel approach of suppressing angiogenesis in TNBC with small molecules that target the PPI between CRYAB and VEGF. There is a critical need for targeted therapies in TNBC since the only established treatment for this aggressive disease is chemotherapy, which has been shown to be ineffective in terms of medium- to long-term survival. Angiogenesis is one of the main targets in TNBC due to its role in disease progression, however, most anti-angiogenic therapies have shown mixed and sometimes disappointing results. In the tumour microenvironment, CRYAB is a chaperone protein that has been shown to bind to and correct unfolded/misfolded VEGF promoting angiogenesis. This protein is overexpressed in TNBC and has been found to correlate with poor prognosis in this disease setting, making it an attractive target for the development of new anti-angiogenic therapies. Several studies looking at the interaction between CRYAB and regulator proteins identified a “hotspot” on the surface of CRYAB where VEGF interacts. Aided by molecular docking methods, small molecule hit compounds were identified which bind to this “hotspot” and could potentially inhibit this PPI.

In this paper, we report a proof-of-concept study devised to validate this target. The work started with the synthesis of novel purine-based compounds for structural activity relationship studies. The newly synthesised analogues were then subjected to biological evaluation, firstly, in a cell viability assay where several of the analogues were found to significantly reduce the viability of MDA-MB-231 and MDA-MB-436 TNBC cell lines. The most potent of these analogues were then tested for their ability to disrupt the CRYAB/VEGF interaction in a custom designed cell-based CRYAB/VEGF₁₆₅ PPI assay. The PPI assay showed that compounds **4e** and **4f** successfully disrupted the interaction between CRYAB and VEGF₁₆₅. Additionally compound **4e** (100 μ M) was found to decrease the amount of VEGF secreted by MDA-MB231 TNBC cells by 40%. Molecular docking studies also suggested that these two analogues interfere with the target “hotspot” through key interactions with specific amino acids. In conclusion, for this work to progress to pre-clinical trials as a viable therapeutic option in TNBC, further design, synthesis and in vitro studies are required to validate this novel concept. Additional studies on lead compound stability and other pharmacokinetic properties will also be required prior to evaluation within relevant in vivo models and identification of a new pre-clinical drug candidate.

Acknowledgements We thank Cancer Research Wales for a post-doctoral research associate award (to NF-M), and acknowledge the EPSRC UK National Mass Spectrometry Facility at Swansea University for provision of mass spectrometry analysis. We thank Essen BioScience for providing IncuCyte™ live-cell imaging system and reagents for cytotoxicity measurements.

Compliance with ethical standards

Conflict of interest The authors declare that they have no conflict of interest.

Publisher's note: Springer Nature remains neutral with regard to jurisdictional claims in published maps and institutional affiliations.

Open Access This article is distributed under the terms of the Creative Commons Attribution 4.0 International License (<http://creativecommons.org/licenses/by/4.0/>), which permits use, duplication, adaptation, distribution, and reproduction in any medium or format, as long as you give appropriate credit to the original author(s) and the source, provide a link to the Creative Commons license, and indicate if changes were made.

References

- Arkin MR, Tang YY, Wells JA (2014) Small-molecule inhibitors of protein-protein interactions: progressing toward the reality. *Chem Biol* 21:1102–1114
- Arrigo AP, Simon S, Gibert B, Kretz-Remy C, Nivon M, Czekała A, Guillet D, Moulin M, Diaz-Latoud C, Vicart P (2007) Hsp27 (HspB1) and alpha B-crystallin (HspB5) as therapeutic targets. *FEBS Lett* 581:3665–3674
- Banerjee A, Lang JY, Hung MC, Sengupta K, Banerjee SK, Baksi K, Banerjee DK (2011) Unfolded protein response is required in nu/nu mice microvasculature for treating breast tumor with tunicamycin. *J Biol Chem* 286:29127–29138
- Bear HD, Tang G, Rastogi P, Geyer Jr. CE, Robidoux A, Atkins JN, Baez-Diaz L, Brufsky AM, Mehta RS, Fehrenbacher L, Young JA, Senecal FM, Gaur R, Margolese RG, Adams PT, Gross HM, Costantino JP, Swain SM, Mamounas EP, Wolmark N (2012) Bevacizumab added to neoadjuvant chemotherapy for breast cancer. *New Eng J Med* 366:310–320
- Biagi G, Costantini A, Costantino L, Giorgi I, Livi O, Pecorari P, Rinaldi M, Scartoni V (1996) Synthesis and biological evaluation of new imidazole, pyrimidine and purine derivatives and analogs as inhibitors of xanthine oxidase. *J Med Chem* 39:2529–2535
- Chen ZJ, Ruan Q, Han S, Xi L, Jiang WG, Jiang HB, Ostrov DA, Cai J (2014) Discovery of structure-based small molecule inhibitor of alpha B-crystallin against basal-like/triple-negative breast cancer development in vitro and in vivo. *Breast Cancer Res Treat* 145:45–69
- Cheng CC, Robins RK (1958) Potential purine antagonists. 12. Synthesis of 1-alkyl(aryl)-4,6-disubstituted pyrazolo[3,4-d]pyrimidines. *J Org Chem* 23:852
- Chhabra S, Barlow N, Dolezal O, Hattarki MK, Newman J, Peat TS, Graham B, Swarbrick JD (2013) Exploring the chemical space around 8-mercaptopurine as a route to new inhibitors of the folate biosynthesis enzyme HPPK. *PLoS ONE* 8:e59535
- Corder AL, Subedi BP, Zhang SA, Dark AM, Foss FW, Pierce BS (2013) Peroxide-shunt substrate-specificity for the Salmonella typhimurium O-2-dependent tRNA modifying monooxygenase (MiaE). *Biochem* 52:6182–6196
- De Azevedo WF, Leclerc S, Meijer L, Havlicek L, Strnad M (1997) Inhibition of cyclin-dependent kinases by purine analogues: crystal structure of human cdk2 complexed with roscovitine. *FEBS J* 243:518–526
- Essen Bioscience. IncuCyte™ cytotoxicity assay general protocol. <https://www.essenbioscience.com/en/applications/cell-health-via-bility/cytotoxicity>. Accessed 5th December 2017
- Fosu-Mensah N, Peris MS, Weeks HP, Cai J, Westwell AD (2015) Advances in small molecule drug discovery for triple-negative breast cancer. *Fut Med Chem* 7:2019–2039
- Garrido C, Paul C, Seigneuric R, Kampinga HH (2012) The small heat shock family proteins family: the long forgotten chaperones. *Int J Biochem Cell Bio* 44:1588–1592
- Ghanem H, Jabbour E, Faderl S, Ghandi V, Plunkett W, Kantarjian H (2010) Clofarabine in leukemia. *Exp Rev Hematol* 3:15–22
- Ghosh JG, Shenoy AK, Clark JI (2007) Interactions between important regulatory proteins and human alpha B crystallin. *Biochem* 46:6308–6317
- Gonçalves DC, Marin TM, Pereira MBM, Santos AM, Leme AFP, Franchini KG (2016) Alpha B-crystallin interacts and attenuates the tyrosine phosphatase activity of Shp2 in cardiomyocytes under mechanical stress. *FEBS Lett* 590:2232–2240
- Goosin M (2011) Avastin hearing leads to more uncertainty over drug's future. *J Natl Cancer Inst* 103:1148–1150
- Haynes B, Zhang YH, Liu FC, Li J, Petit S, Kothayer H, Bao X, Westwell AD, Mao GZ, Shekhar MPV (2016) Gold nanoparticle conjugated Rad6 inhibitor induces cell death in triple negative breast cancer cells by inducing mitochondrial dysfunction and PARP-1 hyperactivation: synthesis and characterization. *Nanomed: Nanotech Biol & Med* 12:745–757
- Ibrahim N, Legraverend M (2009) High-yielding two-step synthesis of 6,8-disubstituted N-9-unprotected purines. *J Comb Chem* 11:658–666
- Jehle S, Rajagopal P, Bardiaux B, Markovic S, Kühne R, Stout JR, Hignman VA, Klevit RE, van Rossum BJ, Oschkinat H (2010) Solid state NMR and SAXS studies provide a structural basis for the activation of alpha B-crystallin oligomers. *Nat Struct Mol Biol* 17:1037–1042
- Johnston TP, Holum LB, Montgomery JA (1958) Synthesis of potential anticancer agents. 16. S-substituted derivatives of 6-mercaptopurine. *J Am Chem Soc* 80:6265–6271
- Joule JA, Mills K, Smith GF (1995) *Heterocyclic chemistry*, 3rd edn. Wiley-Blackwell, London
- Kim LS, Huang S, Lu WX, Lev DC, Price JE (2004) Vascular endothelial growth factor expression promotes the growth of breast cancer brain metastases in nude mice. *Clin Exp Metastasis* 21:107–118
- Launay N, Tarze A, Vicart P, Lilienbaum A (2010) Serine 59 phosphorylation of alpha B-crystallin down-regulates its anti-apoptotic function by binding and sequestering Bcl-2 in breast cancer cells. *J Biol Chem* 285:37324–37332
- Lehmann BD, Bauer JA, Chen X, Sanders ME, Chakravarthy AB, Shyr Y, Pietenpol JA (2011) Identification of human triple-negative breast cancer subtypes and preclinical models for selection of targeted therapies. *J Clin Invest* 121:2750–2767
- Lee JS, Kim HY, Jeong NY, Lee SY, Yoon YG, Choi YH, Yan C, Chu IS, Koh H, Park HT, Yoo YH (2012) Expression of alpha B-crystallin overrides the anti-apoptotic activity of XIAP. *Neuro Oncol* 14:1332–1345
- Levin G, Kalmus A, Bergmann F (1960) Synthesis of 6-thiouric acid and its derivatives. *J Org Chem* 25:1752–1754
- Mayer IA, Abramson VG, Lehmann BD, Pietenpol JA (2014) New strategies for triple-negative breast cancer – deciphering the heterogeneity. *Clin Cancer Res* 20:782–790
- Michael MA, Cottam HB, Smee DF, Robins RK, Kini GD (1993) Alkylpurines as immune potentiating agents – synthesis and antiviral activity of certain alkylguanines. *J Med Chem* 36:3431–3436
- MOE: Molecular Operating Environment - Chemical Computing Group. *Molecular Operating Environment user manual*. https://www.chemcomp.com/MOE-Molecular_Operating_Environment.htm. Accessed 9th February 2017

- Montgomery JA, Hewson K, Clayton SJ, Thomas HJ (1966) Further studies on alkylation of purines. *J Org Chem* 31:2202
- Morrison LE, Hoover HE, Thuerauf DJ, Glembotski CC (2003) Mimicking phosphorylation of alpha B-crystallin on serine-59 is necessary and sufficient to provide maximal protection of cardiac myocytes from apoptosis. *Circ Res* 92:203–211
- Mosmann T (1983) Rapid colorimetric assay for cellular growth and survival – application to proliferation and cytotoxicity assays. *J Immunol Methods* 65:55–63
- O'Reilly EA, Gubbins L, Sharma S, Tully RM, Guang MHZ, Weiner-Gorzel K, McCaffrey J, Harrison M, Furlong F, Kell M, McCann A (2015) The fate of chemoresistance in triple negative breast cancer (TNBC). *BBA Clin* 3:257–275
- O'Shaughnessy J, Dieras V, Glaspy J, Brufsky A, Miller KD, Miles DW, Koralewski P, Phan SC, Bhattacharya S (2009) Comparison of subgroup analyses of PFS from three Phase III studies of bevacizumab in combination with chemotherapy in patients with HER2-negative metastatic breast cancer. *Cancer Res* 69:512S
- Pathak AK, Pathak V, Seitz LE, Suling WJ, Reynolds RC (2004) Antimycobacterial agents. 1. Thio analogues of purine. *J Med Chem* 47:273–276
- Pereira MBM, Santos AM, Gonçalves DC, Cardoso AC, Consonni SR, Gozzo FC, Oliveira PS, Pereira AHM, Figueiredo AR, Tirolip Cepeda AO, Ramos CHI, de Thomaz AA, Cesar CL, Franchini KG (2014) α B-crystallin interacts with and prevents stress-activated proteolysis of focal adhesion kinase by calpain in cardiomyocytes. *Nat Commun* 5:5159
- Ranpura V, Hapani S, Wu S (2011) Treatment-related mortality with bevacizumab in cancer patients. *J Am Med Assoc* 305:487–494
- Robins RK (1957) Potential purine antagonists. 9. Further studies of some 4,6-disubstituted pyrazolo[3,4-d]pyrimidines. *J Am Chem Soc* 79:6407–6415
- Robins RK (1958) Potential purine antagonists. 15. Preparation of some 6,8-disubstituted purines. *J Am Chem Soc* 80:6671–6679
- Rodriguez G (1994) Fludarabine phosphate – a new anticancer drug with significant activity in patients with chronic lymphocytic leukemia and in patients with lymphoma. *Inv New Drugs* 12:75–92
- Ruan Q, Han S, Jiang WG, Boulton ME, Chen ZJ, Law BK, Cai J (2011) Alpha B-crystallin, an effector of unfolded protein response, confers anti-VEGF resistance to breast cancer via maintenance of intracrine VEGF in endothelial cells. *Mol Cancer Res* 9:1632–1643
- Sahasranaman S, Howard D, Roy S (2008) Clinical pharmacology and pharmacogenetics of thiopurines. *Eur J Clin Pharmacol* 64:753–767
- Steeg PS (2006) Tumor metastasis: mechanistic insights and clinical challenges. *Nat Med* 12:895–904
- Tsang JYS, Lai MWH, Wong KHY, Chan SK, Lam CCF, Tsang AKH, Yu AMC, Tan PH, Tse GM (2012) Alpha-B-crystallin is a useful marker for triple negative and basal breast cancers. *Histo-pathol* 61:378–386
- Veronesi V, Flouquet N, Farce A, Carato P, Leonce S, Pfeiffer B, Berthelot P, Lebegue N (2010) Synthesis, biological evaluation and docking studies of 4-amino-tetrahydroquinazolino[3,2-e] purine derivatives. *Eur J Med Chem* 45:5678–5684
- Villatoro MJPDY, Unciti-Broceta JD, Contreras-Montoya R, Garcia-Salcedo JA, Mezo MAG, Unciti-Broceta A, Diaz-Mochon JJ (2015) Amide-controlled, one-pot synthesis of tri-substituted purines generates structural diversity and analogues with trypanocidal activity. *Sci Rep* 5:9139
- von Minckwitz G, Eidtmann H, Rezai M, Fasching PA, Tesch H, Eggemann H, Schrader I, Kittel K, Hanusch C, Kreienberg R, Solbach C, Gerber B, Jackisch C, Kunz G, Blohmer J-U, Huober J, Hauschild M, Fehm T, Müller BM, Denkert C, Loibl S, Nekljudova V, Untch M (2012) Neoadjuvant chemotherapy and bevacizumab for HER2-negative breast cancer. *New Eng. J Med* 366:299–309
- White AW, Westwell AD, Brahehi G (2008) Protein-protein interactions as targets for small-molecule therapeutics in cancer. *Expert Rev Mol Med* 10:e8
- Yang JX, Dang Q, Liu JL, Wei ZL, Wu JC, Bai X (2005) Preparation of a fully substituted purine library. *J Comb Chem* 7:474–482